Applied Surface Science Advances 6 (2021) 100163

Contents lists available at ScienceDirect

Applied Surface Science Advances

journal homepage: www.sciencedirect.com/journal/applied-surface-science-advances

Magnetic nanoparticles in biomedical applications: A review

Elsa M. Materón [a], Celina M. Miyazaki [b], Olivia Carr [a], Nirav Joshi [a], Paulo H.S. Picciani [c], Cleocir J. Dalmaschio [d], Frank Davis [e], Flavio M. Shimizu [f,*]

[a] São Carlos Institute of Physics, University of São Paulo, CP 369, São Carlos, SP 13560-970, Brazil
[b] Department of Physics, Chemistry and Mathematics, Federal University of São Carlos, Rod João Leme dos Santos, km 110, Sorocaba, SP 18052-780, Brazil
[c] Instituto de Macromoléculas Professora Eloisa Mano, Universidade Federal do Rio de Janeiro (IMA/UFRJ), Rio de Janeiro, RJ 21941-598, Brazil
[d] Department of Chemistry, Federal University of Espírito Santo, Vitória, ES 29075-910, Brazil
[e] Department of Engineering and Applied Design, University of Chichester, Bognor Regis, West Sussex PO211HR, UK
[f] Department of Applied Physics, "Gleb Wataghin" Institute of Physics (IFGW), University of Campinas (UNICAMP), Campinas, SP 13083-859, Brazil

ARTICLE INFO

Keywords:
Magnetic nanoparticles
Chronic diseases
Immunoassays
Biomedical applications

ABSTRACT

Biomedical applications with emphasis on the design of smart materials, specifically magnetic nanoparticles (MNPs) are considered to have technological benefits because they can be manipulated using magnetic fields. Magnetic NPs have been widely used in hyperthermia, target drug delivery system, imaging, and extraction of biomolecules, postulating them also as an important tool in cancer treatment. Morphological structures of magnetic materials have drawn tremendous attention from diverse scientific fields due to their unique surface chemistry, nontoxicity, biocompatibility, and particularly their inducible magnetic moment. This review features recent research accomplishments made in the biomedical field using magnetic nanoparticles. The first part gives a comprehensive overview of magnetic nanoparticles in the treatment of chronic diseases and drug targeting. The second part includes the role of magnetic nanoparticles in electrochemical, optical-based immunoassays. The review also outlines the current challenges and future research perspectives for fostering advanced and high-performance magnetic nanoparticles in technological applications.

1. Introduction

The convergence of nanotechnology with molecular biology and medicine has led to the active development of a modern evolving field of study, nanobiotechnology, which provides exciting opportunities to discover novel materials, processes, and phenomena. In the 1950s, Gilchrist et al. treated lymphatic nodes and metastases by injecting metallic particles heated by a magnetic field [1]. Shortly after that, magnetic nanoparticles (MNPs) were increasingly introduced into drug delivery, enzyme immobilization [2], and empowered a plethora of exciting biotechnological applications. There are interesting characteristics such as size uniformity, high surface area, biocompatibility [3,4], superparamagnetism, adsorption kinetics, and magnetic moment that can be tailored during the production process for specific applications [5]. Among various types of nanoparticles, iron oxide nanoparticles have been widely explored by researchers because it does not retain any magnetization when the magnetic field is removed. In fact, iron oxide nanoparticles (Fe_3O_4 and Fe_2O_3) have been widely applied for *in vitro* diagnosis and even now for other applications due to their easy functionalization with polymers and other materials.

Different methods are available to fabricate magnetic nanostructures in the form of nanorods, nanowires, nanocubes, including iron oxide magnetic nanoparticles that can be prepared by several different preparation methods, including wet chemistry or "bottom-up" routes such as hydrothermal, solvothermal, sol-gel, co-precipitation, flow injection syntheses, electrochemical, and laser pyrolysis techniques [6]. Similarly, the biosynthesis of magnetic nanoparticles have been explored [7,8]. Detailed reviews on the synthesis of magnetic nanoparticles has been reported earlier in [9,10]. With efficient control over particle size, hydrolytic and nonhydrolytic wet chemistry procedures have shown promising outcomes. Similarly, in manufacturing fine powders with an average particles size of 20–50 nm, the new laser ablation, evaporation synthesis, and microbial method has been reported as effective route preparation [11]. The magnetic field parameter plays an essential role in MNP cytotoxicity, the most significant of which are magnetic field amplitude, frequency, and the duration of action [12]. The literature reports that large MNP presents a cytotoxic effect in alternating low-frequency magnetic fields (LF AMF) than smaller ones [13]. The

* Corresponding author.
E-mail address: fshimizu@unicamp.br (F.M. Shimizu).

https://doi.org/10.1016/j.apsadv.2021.100163
Received 3 April 2021; Received in revised form 26 August 2021; Accepted 4 September 2021
Available online 14 September 2021

particle size should be small enough (< 200 nm) to avoid being sequestrated from blood, where they accumulate and are expelled through the hepatic filtration and mononuclear phagocyte system, but large enough (> 10 nm) to avoid renal filtration and rapid penetration [11,14,15].

Strategies to improve some properties like biocompatibility, poor biodegradability and chemical instability in a physiological environment rely on surface modification of MNPS and superparamagnetic iron oxide nanoparticles (SPIONS) [15,16]. The surface of MNPS has been functionalized covalently with biodegradable and biocompatible polymers [17,18] such as polysaccharides [19,20,21] and linoleic acid [22]. There are also two kinds of functionalization strategies: molecular functionalization that combine magnetic nanomaterials with other functional nanostructures by sequential growth or coating, as depicted in **Fig. 1**. First, biofunctional molecules such as antibodies, ligands, or receptors coating magnetic nanoparticles and make them interact with biological entities with high affinity, thus providing a controllable means of "tagging" and confer high selectivity and sensitivity for many biological applications. Secondly, the integration of magnetic nanoparticles with other material (e.g., metallic nanoparticles), can form heterodimer structures that offer distinct surfaces and properties to allow different kinds of functional molecules that attach onto the specific parts of the heterodimers, which may bind to multiple receptors or act as agents for multimodality imaging [23], serving also as platforms for bacteria detection [24,25] and therapeutic agent [26].

In the last few years, a plethora of articles have been published on the biomedical application using magnetic materials. However, very few works on the treatment of chronic diseases such as cancer were found. Instead, interesting reviews cover the following aspects, (*i*) developments of hydrogel devices for biomedical applications and practical issues arising during synthesis, modeling, or use [27], (*ii*) recent advances in the field of biomedicine using iron oxide and its derivatives [28], (*iii*) detailed study on the synthesis, properties of magnetic nanoparticles, biofunctionalization and technological application of such magnetic NPs in hyperthermia, drug release, tissue engineering, theragnostic, and lab-on-a-chip [29]. Hence, it is imperative to acutely unfold the various design strategies of magnetic nanoparticles with a holistic overview of their application in electrochemical, optical-based immunoassays, and in the treatment of drug targeting. An effort to highlight the current advancements is focused on two main topics. First is the use of MNPs as a key tool in the treatment of chronic diseases such as cancer, which through hyperthermia treatment may induce antitumoral immunity [30,31]. Cytotoxic drugs used in cancer treatment are nonselective and can cause damage in normal tissues, although cancer cells are innately more vulnerable than normal cells to the effect of such drugs. Nanoparticles are strategically designed with dimensions similar to biological vesicles or molecules found in our body and that; these can pass through blood vessels to safely reach their target and eventually release their cargo at the site of the disease. The main advantage of magnetic nanoparticles lies in controlling their distal location or thermal activation by applying alternating magnetic fields (kHz-MHz) that do not cause adverse effects to the human body [31]. This favors obtaining stable colloids and can be easily passaged or accumulate into several tumors, allowing the administration of drug delivery for different routes, including brain tumors, and can cross the blood-brain barrier (BBB) effectively. Similarly, in recent studies, MNPs have filtered cancer cells attached to the nanoparticle surface, and these conjugates were carried out of the body [31–33], as a strategy to avoid bioaccumulation issues. In contrast to metallic nanoparticles, which are photothermally activated by near-infrared (NIR) light and some present antimicrobial properties [34] and have no control over their distal location, harming their therapeutic efficiency. Moreover, their presence in the environmental or biological systems can cause adverse effects on human health and ecological biodiversity due to the cytotoxic properties of metal [35]. These are some of the main challenges under investigation for the use of metallic nanoparticles as a therapeutic agent. The second is intended to discuss the recent advances in the development of biosensors for rapid detection of a wide variety of clinical conditions without the need for extensive laboratory-based testing. More specifically concerning the early diagnosis of diseases, such as cancer, and its strategies for biomolecule capture in complex biological fluid media.

2. MNPs in the treatment of chronic diseases

Chemotherapy agents are mostly designed to act on cancer cells, although they are nonselective and can also cause injury to healthy tissues. Another current obstacle in chemotherapy is the poor aqueous solubility and permeability of anticancer drugs, the difficult bioavailability, and the treatment efficiency [36,37]. Solid tumors have specific characteristics that make them more vulnerable, for example, tumors cannot expand beyond the diffusion limit of nutrients from the nearest capillary, which is approximately 100–500 microns. Then, tumor cells grow by the angiogenesis process, which is not organized. They secrete factors that cause increased vascularization to stimulate vessel growth, motility, and permeability [38]. However, the tumor also can create an area where vascularization is reduced and, subsequently, low drug distribution [39,40]. However, the vessels created have permeable pores up to 1 μm in size and facilitate extravasation of circulating nanoparticles modified with a specific ligand that recognizes tumor-specific receptors into the tumor environment and thus enhanced permeability and retention (EPR) effects. In contrast with healthy cells that possess tightly endothelial cells and do not readily extravasate, avoiding the

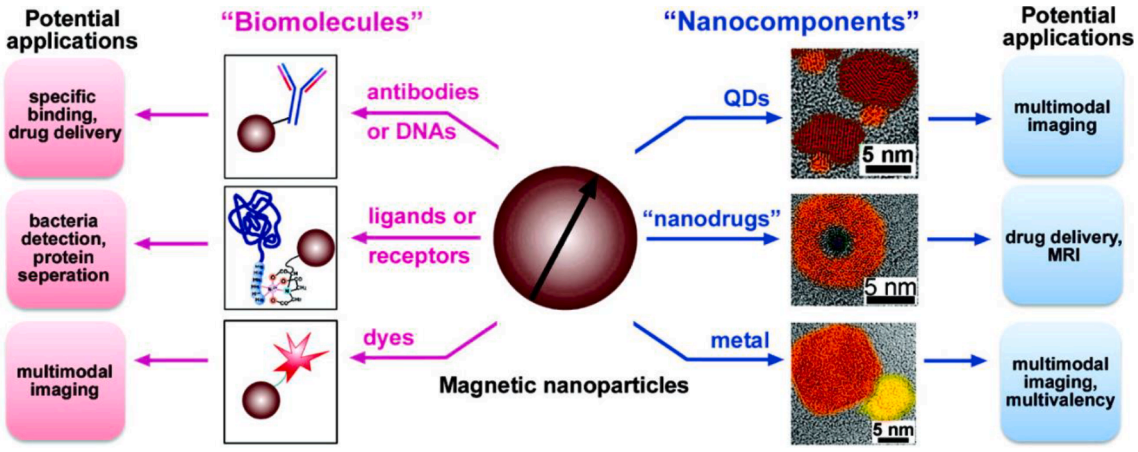

Fig. 1. The scheme illustrates two commonly used strategies to fabricate multifunctional magnetic nanoparticles and their potential applications. Reproduced with permission from [23]

diffusion of NPs from the blood vessels [41–46]. In vascular-rich tumors, the efficacy of nanoparticle-mediated drug delivery should be higher in comparison to hypovascular ones [47]. Notwithstanding, the drug needs to reach hypovascular places. For this reason, the tumor microenvironment should be altered with specific chemotherapeutic agents such as nitroglycerin (glyceryl trinitrate), and S-1 [47]. Certainly, nanoparticles are considered a promising tool for improved pharmacokinetics and pharmacodynamics of drugs widely used in cancer treatments [36,47,48]. Due to the ability to synthesize nanoparticles in different shapes and sizes, the high encapsulation, reduced toxicity, stability, efficacy, specificity, the capacity to incorporate both hydrophilic and hydrophobic drugs, and tolerability of drug-loaded nanoparticles, and they can enter the capillary pores of cancer cells; hence, increasing the drug concentrations, specifically in the targeted cancer cell [36,49,50]. Also, nanoparticles can be synthesized from a wide range of precursor materials, such as lipids (*e.g.*, solid lipid nanoparticles, liposomes), polymers (*e.g.*, polymeric nanoparticles), and inorganic materials (*e.g.*, gold nanoparticles) [36,43].

2.1. Drug targeting

A suitable biological nanocarrier must have the following characteristics: bio-compatibility, easiness of surface modification, high encapsulation efficiency, longer shelf life, easy availability, and cost-effectiveness [51]. The nanocarriers are divided into organic, inorganic, and organo-inorganic hybrids. Organic carriers are mostly liposomes, solid-lipid nanoparticles (SLN), polymeric nanoparticles, and biomimetic virus-based nanoparticles [51]. The first commercial nanoparticles approved for therapy in cancer were the liposomes; Doxyl in the U.S. (Doxorubicin, Caelyx outside the U.S), and DaunoXome (Daunorubicin) [39]. Solid-lipid nanoparticles are spherical and usually have a range from 50 nm to 1 μm. Digestible solid lipids as such as diglycerides, triglycerides, phospholipids, and fatty acids are commonly used in the synthesis of these nanoparticles. The SLNs have several advantages such as; facile delivery of active agents to tumors, suppressed resistance, the capacity of regulating drug exposure, and synergistic effects of mixed cargo [51,52]. Senthil Kumar et al. evaluate the efficacy of chitosan-coated-trans-resveratrol and ferulic acid-loaded SLNs, in which the authors conjugated with folic acid for colon cancer treatment. According to the authors, SLNs showed good stability under acidic conditions and increased cytotoxicity in cancer cells [52]. Li et al. synthesized nanoparticles based on phospholipid complex 1,2-distearoyl-sn-glycero-3-phosphoethanolamine-N-[methoxy (polyethylene glycol)-2000]-folate (DSPE-PEG-FA) for drug delivery of mitomycin C (MMC) [53]. Also, polymeric nanoparticles were prepared with a size between 10nm and 1000nm using chitosan, poly(lactide-co-glycolide), poly(lactic acid), polyacrylic acid, and alginate [54]. Polymer nanoparticles are usually synthesized by methodologies like solvent evaporation, salting out and dialysis [51]. Most related polymeric nanoparticles are considered biocompatible, provide protection against drug degradation, are non-immunogenic, have high encapsulation efficiency of lipophilic drugs, and can be quickly eliminated from the organism [51,55]. Abriata et al. [55], developed a polymeric nanoparticle system based on poly-e-caprolactone (PCL) for paclitaxel drug, which is widely used in ovarian cancer treatment. *In vitro* studies have shown good release of drugs and reduced cell viability for SKOV-3 cell lines.

Inorganic nanoparticles of the size range of 10 nm to 500 nm with spherical or rod shapes based on gold, silver, silica, and iron are usually modified with different chemical groups that facilitate their conjugation with antibodies, ligands, and other drugs [51]. Nanoparticles can reach specific targets by the active process into tumoral tissues, mostly due to modification with specific antibodies or biomolecules able to interact with specific receptors in target cells [39]. Mesoporous inorganic materials have been incorporated and reported to interact effectively with soluble drugs [56]. Nan Lu and co-workers developed thioether-bridged periodic mesoporous organosilica nanoparticles (PMOs) modified with Cy5,5 and anti-Her2, which could be used for cancer cell targeting imaging and drug delivery of doxorubicin. Also, the developed nanoparticles have shown dual-responsive drug delivery for glutathione and pH [57].

Furthermore, nanoparticles based on metal elements gold, zinc [58], cobalt, manganese [59], and also magnetic nanoparticles are widely used to contribute to the heating efficiency for hyperthermic treatment [60]. This treatment consists of heating tumor cells to a temperature range of 40–45 ºC, which is enough to destroy or induce apoptosis in cancer cells, once normal cells can tolerate elevated temperatures [61–65]. Magnetic fluid hyperthermia (MFH) and photothermal therapy (PTT) have been widely used for the treatment of cancer. MFH is based on the use of an external alternating magnetic field (AMF) to drive magnetic nanoparticles to different directions and, consequently, heat release in comparison to PTT uses photoabsorbing agents to generate heat from light [66]. Also, photodynamic therapy (PDT) usually uses singlet oxygen (SO) or reactive oxygen species (ROS) generated from photosensitizer (PS) molecules under light exposure [61,67]. The literature reported the use of magnetic nanoparticles where nanoparticles first give 42 °C of hyperthermia to the tumor and additionally catalyze the generation of highly toxic reactive oxygen species (ROS) **(**Fig. 2**a)** [68]. Furthermore, Chan Ming-Hsien et al. developed magnetic fluid hyperthermia (MFH) based on FePt nanoparticles with kaolinite modified with cetyltrimethylammonium bromide (CTAB) as exhibited in Fig. 2**b.** The nanocomposites showed promise for loading the drug doxorubicin and could be used as a tool in magnetic resonance imaging (MRI) to guided targeting [69].

Fig. 3**a** shows the research work reported by Liu et al. a magneto thermodynamic (MTD) therapy by combined reactive oxygen species and heating effect [70]. The authors developed ferrimagnetic vortex-domain iron oxide nanoring and graphene oxide (FVIOs-GO) hybrid nanoparticles that showed strong immune response at physiological temperatures, below 40 °C, in the hypoxic tumor microenvironment by a notably amplified ROS level under alternating magnetic field (AMF) [70]. Wang et al. proposed block copolymer micelles containing hyaluronic acid (HA) and Mn-Zn ferrite magnetic nanoparticles (MZF) to increase the therapeutic effect of radiotherapy for the treatment of lung cancer (Fig. 3**b**) [71].

2.2. Magnetic drug targeting/magnetic hyperthermia

Hyperthermia is not the unique application of magnetic nanoparticles studied in cancer therapy. Researchers have also been exploiting the enhancements in drug delivery field, which allows a better control not only for guiding the carriers but also the release of the drugs upon reaching the tumor site [72]. This is possible due to external triggering of the magnetic field [73]. Moreover, such strategy allows to incorporate anticancer chemotherapeutic drug from single up to multi-chemotherapeutic agents [74]. Due to the wide range of possibilities to combine multiple functions in cancer therapy, there is a grown interest on magnetic nanoparticles for application in cancer treatments.

Since then, novel methodologies based on the combination of different treatments have been developed, one of them is the combination of photothermal, drug target, and PDT. Li et al. synthesized mesoporous carbon nanoparticles modified with lipid bilayers. This thermo-chemotherapy system contains doxorubicin drugs to enhance permeability and retention (EPR) effects caused by NIR light exhibited a synergistic therapeutic efficiency for cancer cells. According to the authors, tumor local temperature reached up to 51.9 ºC 3 min after exposure to laser at intensity of 1.25 W cm^{-2} [75]. Copper sulfide doped periodic mesoporous organosilica nanoparticles (CuS@PMOs) have also been used in hyperthermia and drug delivery of doxorubicin. The system of drug release is controlled by three stimuli: intracellular glutathione (GSH), acidic environment in tumor cells, and external laser irradiation [76]. Millers et al., attached monomethyl auristatin E (MMAE), a potent mitotic inhibitor, and doxorubicin to the palladium nanoparticles with a

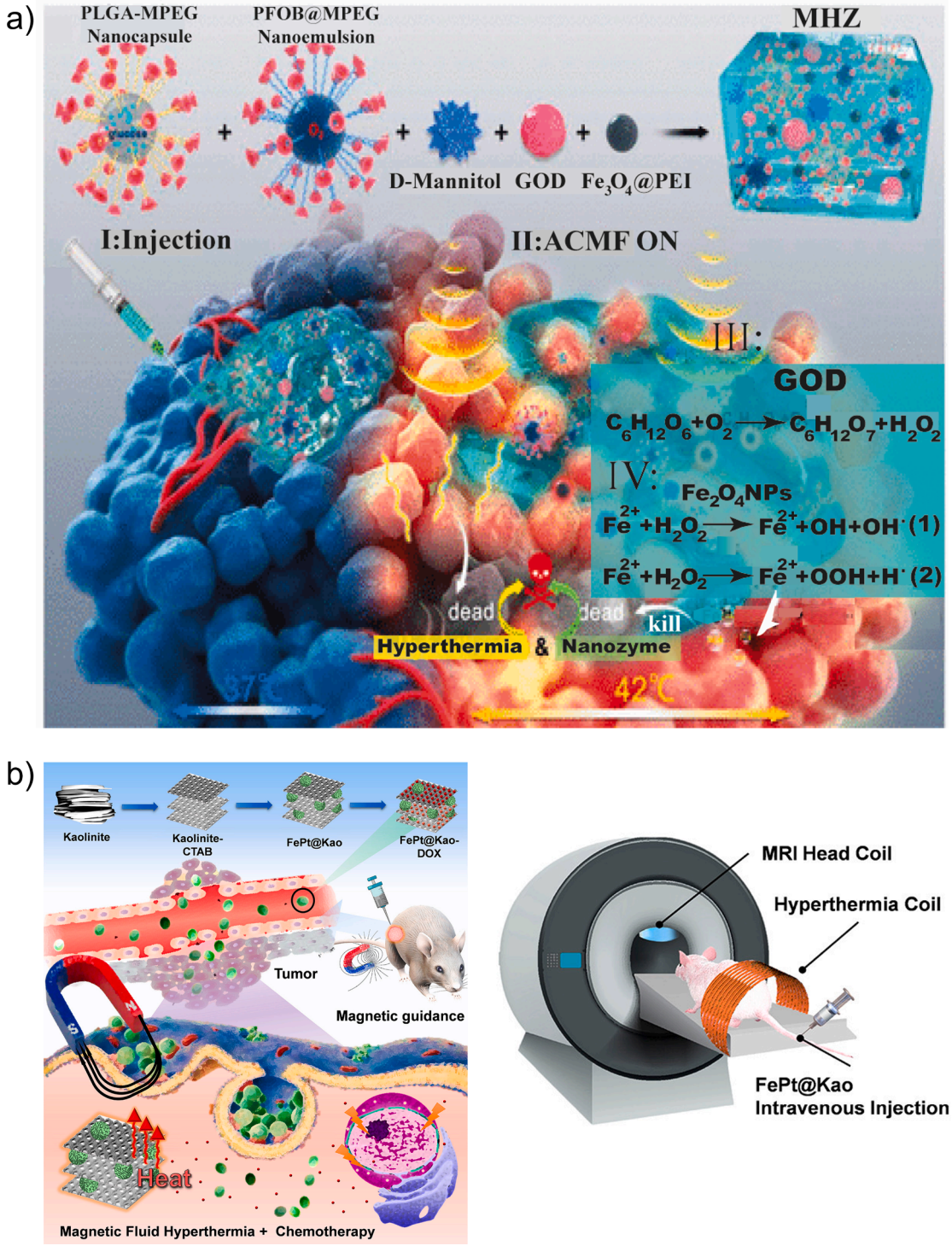

Fig. 2. Illustration of (a). The design exhibited the synergistic Magnetic hyperthermia (MHZ) and ROS for cancer therapy. Modified with permission from [68]. (b) system of Doxorubicin loaded FePt nanoparticles combined with kaolinite modified with cetyltrimethylammonium bromide (CTAB), (FePt@Kao-Dox). Modified with permission from [69].

size of 60 nm, by alkyl chain immobilization [77]. Additionally, the authors used single low-dose radiation to increase EPR combined with the prodrug strategy, which produces synergistic effects on tumoral reductions [77]. Table 1 summarizes the most popular magnetic nanoparticles used in combination to drug and applied in hyperthermia for cancer treatments.

3. Recent advances MNPs in immunoassays

Promising alternatives for analytical techniques widely explored in the literature are electrochemical immunosensors since they combine the high sensitivity and selectivity of traditional immunoassay methods with simpler operating regimes [120]. Electrochemical transducers can be categorized into four measurement techniques: potentiometric, conductometric, amperometric, and impedance spectroscopy [121].

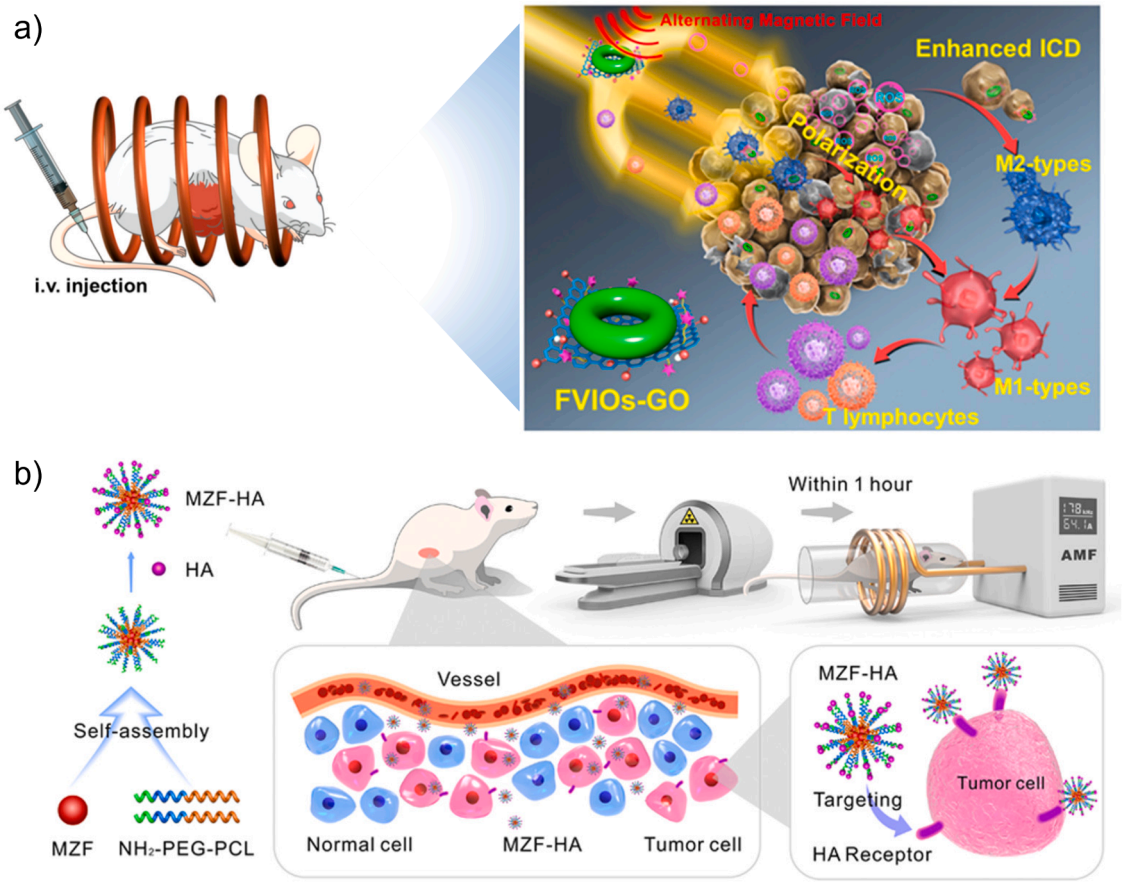

Fig. 3. Schematic designer of (a) systemicatic delivery magnetic nanothermia experiment and mechanism of action of FVIOs-GO at a physiological tolerated temperature. Modified with permission from [70]. (b). Schematic illustration of Mn-Zn ferrite magnetic nanoparticles modified with hyaluronic acids for cancer treatment. Reproduced with permission from [71].

These methods usually offer advantages over traditional laboratory methods such as rapid response, reduced costs, portability, and the relative ease of many microfabrication technologies [122].

World Health Organization (WHO) defined biomarkers as "any substance, structure, or process that can be measured in the body or its products and influence or predict the incidence of outcome or disease" [123]. The main biomarkers employed for the clinical diagnosis of diseases, such as cancer, include enzymes, DNA, RNA, and proteins. In general, these biological components are present in our body at low levels, especially during the early stages of the disease, which often makes necessary a sample preparation step to separate/-purify/preconcentrate the biomarker to be detected from a biological fluid that is a complex matrix with a range of biological elements. These can act as interferents which can greatly complicate target detection. These requirements rule the projects for the creation of sensitive and selective tools for detecting these biomarkers. A promising strategy to accomplish such requirements is based on the use of magnetic nanoparticles (MNPs), which have been widely studied within the development of immunoassays due to their high stability, small size, rapid reaction kinetics, and ease of surface modification of the MNPs with a range of functional groups. This facilitates their functionalization with biological components such as DNA, RNA, enzymes, streptavidin, and proteins [124]. MNPs are mainly formed by iron oxides such as magnetite (Fe_3O_4), maghemite (α-Fe_2O_3), and hematite (Fe_2O_3) [125]. In general, methods for synthesizing magnetite nanoparticles include such widely used strategies as ultrasonic irradiation, sol-gel, thermal decomposition, and coprecipitation [126].

Many reviews have been written on a variety of topics related to the use of magnetic nanoparticles in electrochemical immunoassays [121, 127–132]. They mainly discuss applications for MNPs such as clinical marker assays, environmental, and food analysis. Overall, contributions describing the use of magnetic nanoparticles within immunoassays efforts have been driven into:

I Sample preparation: this family of nanoparticles can be used for the magnetic separation of biomarkers of interest from biological matrices (blood, saliva, etc) with an efficiency comparable with immunoaffinity columns and do not require advanced equipment such as centrifuges, filtration systems, chromatographic instruments [130,133].

II Biomarkers: the search for novel biomarkers is still a challenge for the improvement of diagnosis.

III Immunosensors: MNPs have been widely explored as a material for immobilizing proteins and enzymes, and also to be used as a tag for signal amplification or enzyme mimicking [127]. This strategy implies the use of nano- and microparticles as a means of immobilizing biomarkers and, consequently, amplifying the analytical signal. Furthermore, it facilitates the capture and separation of the analyte, due to its magnetic properties. This allows both preconcentration and the elimination of possible interferents, minimizing the matrix effect creating an appropriate label for the assays [127,134,135]. In this topic, we will focus on recent advances in addressing the last two challenges.

The possibility of MNPs functionalization with amino and carboxylic groups allows their modification with a range of biomarkers. Sandwich type immunoassays using MNPs present many advantages over conventional sandwich assays, such as ELISA, mainly due to the possibility

Table 1
Magnetic nanoparticles used in combination of different treatments to increase the efficiency of cancer therapy.

Drug name	Nanoparticles	Ref.
Acyclovir	Fe_3O_4 Magnetic nanoparticles	[78]
Magnetic drug targeting/ magnetic hyperthermia/ targeting delivery	Magnetic nanoparticles(Fe_3O_4)	[79]
Doxorubicin	methoxy poly(ethylene glycol)-grafted carboxymethyl chitosan	[80]
Doxorubicin	Gelatin/Fe_3O_4-Alginate	[81]
Doxorubicin	(Fe_3O_4) magnetic nanoparticles	[73]
Doxorubicin	Magnetic nanoparticle(Fe_3O_4)/ inhomogeneous magnetic pulses	[82]
Doxorubicin	Starch/Octanoic/superparamagnetic iron oxide	[83]
Doxorubicin	superparamagnetic iron oxide nanoparticles (SPIONs)/ poly (lactic-co-glycolic acid) (PLGA)- AS1411 aptamer (Apt) against murine C26 colon carcinoma cells	[84]
Doxorubicin	magnetic iron oxide nanoparticles (MIONs)/hyperthermia therapy/ chemotherapy	[72]
Doxorubicin	Graphene oxide (GO) and magnetic iron oxide nanoparticles (MNPs)	[85]
Doxorubicin	Superparamagnetic iron oxide nanoparticles/ 1,2-distearoyl-sn-glycero-3-phosphoethanolamine-*N*-[methoxy(polyethylene glycol)-2000] (DSPE-PEG2000)	[86]
Doxorubicin	Superparamagnetic iron oxide nanoparticles/copolymer of reducible polyamidoamine(rPAA)/poly(ethylene glycol)(PEG)/dodecyl amine graft	[87]
Erlotinib	Mesoporous magnetic nanoparticles/ folic acid	[88]
Erlotinib	Methotrexate/Chitosan-magnetic nanoparticles ferrofluid/CS copolymer	[89]
Gemcitabine	Magnetic nanoparticles(Fe_3O_4)/ metformin/peptide pHLIP	[90]
Methotrexate	PEG-Chitosan-Iron Oxide nanocomposites/cancer therapy and dual model imaging	[91]
Methotrexate	Magnetic nanoparticles (MNPs) / Fe1 − xMnxFe2O4	[59]
Methotrexate	PLGA magnetic nanoparticles (Fe_3O_4)	[92]
Methotrexate/Doxorubicin	dendritic chitosan grafted mPEG coated (Fe_3O_4) magnetic nanoparticles	[74]
Methotrexate	Folic acid-chitosan-core-shell nanoparticles	[93]
Telmisartan	Magnetic nanoparticles (Fe_3O_4)/ chitosan	[94]
Zidovudine	$NiFe_2O_4$/poly(ethylene glycol)/lipid NPs	[95]
Photothermal effect/ chemotherapy-Doxorubicin	Porous carbon-coated magnetite nanoparticles(Fe_3O_4)/Hyaluronic acid	[96]
Hyperthermia/Doxorubicin	Iron oxide nanocubes	[97]
5-Fluorouracil	Fe_3O_4 glycidyl methacrylate grafted dextran and then N-vinylcaprolactam and N-vinylimidazole monomers	[98]
Hyperthermia	Cobalt-zinc ferrite nanoparticles ($Co_{1-x}Zn_xFe_2O_4$)	[99]
Hyperthermia	$Zn_{0.3}Fe_{2.7}O_4/SiO_2$	[100]
Hyperthermia	Hydroxyapatite coated iron oxide nanoparticle	[101]
Magnetic hyperthermia	Manganese ferrite nanoparticles	[102]
Hyperthermia	Mn-Zn ferrite nanosphere	[103]
Hyperthermia	Magnesium shallow doped γ-Fe2O3 (Mg0.13-γFe2O3)	[104]
Hyperthermia	Polymethylmethacrylate Fe_3O_4	[105]
Hyperthermia	Hydroxypropyl methyl cellulose/ polyvinyl alcohol / Fe_3O_4	[106]
Magnetically mediated energy delivery	iron oxide core/glucose	[107]
Hyperthermia	Magnetic nanoparticles(Fe_3O_4)	[108]
Hyperthermia		[109]
Hyperthermia	Magnetic mesoporous silica nanocarriers	[110]
Hyperthermia	Magnetic nanoparticles(Fe_3O_4)	[110]
Photodynamic therapy/ Hyperthermia	Magnetic nanoparticles (Fe_3O_4)-hyaluronic acid (AHP)	[111]
Radiation therapy	Au/Iron Oxide	[112]
Gemcitabine	Iron oxide nanoparticles/antiCD44 antibody	[113]
Enhanced imaging-guided cancer therapy	Erythrocyte membrane-coated iron nanoparticles	[114]
Magnetically guided drug delivery	Fe_3O_4@Zirconium phosphate core-shell nanoparticles	[115]
Superparamagnetic Hyperthermia	Magnetite nanoparticles (Fe_3O_4)	[116]
Gene therapy	Magnetic nanoparticles (Fe_3O_4)/ polyethyleneimine (PEI)	[117]
Blood-brain barrier	Magnetic nanoparticles(Fe_3O_4)	[118]
Chemo/hyperthermia therapy	Tragacanth gum/polycrylic acid/Fe_3O_4 nanoparticles	[119]

of signal amplification. A relatively large amount of enzymes and antibodies can be immobilized on the solid support due to their large surface area/volume ratio. This approach provides useful signal amplification, thereby improving the performance of any resultant analytical immunoassays [136–138]. In conventional electrochemical immunosensors, the usual ratio between the antibody and enzyme is 1:1. With the use of magnetic particles, the ratio is amplified to potentially thousands of antibodies and thousands of enzymes to an antigen, as reported in the works of Otieno et al. [139].

The most employed biomarkers in immunoassays are proteins (antigen/antibody), enzymes, DNA, and RNA molecules. Recently, extracellular vesicles have gained attention within the literature due to the abundance of bioinformation contained within them and their diversified and complex repertoire of formation. This leads to a range of species that differ in size and origin, such as exosomes, ectosomes, apoptotic bodies, oncosomes, and large oncosomes [140], as shown in Fig. 4. These extracellular vesicles are produced by the cell as part of a complex endosomal secretory pathway, contain mRNA, microRNA, rRNA, tRNA, DNA, lipids, and proteins [141], and are easily found in blood, saliva, urine, semen, etc. Despite the potential of these biological moieties, challenges in sample preparation (isolation) and comprehension of their biomolecular composition (characterization) towards their use in biosensing devices are still under investigation [142]. In this field of research Moura et al. [143–145] have been studied the use of nanovesicles, more specifically exosomes derived from three breast cancer cell lines (MCF7, MDA-MB-231, and SKBR3). Nanovesicles contain CD9, CD63, and CD81 proteins that are general biomarkers for exosomes, as well as CD24, CD44, CD54, CD326, and CD340 which are specific cancer-related molecules. In their initial study, the authors employed a modified ELISA method by incorporating an immunomagnetic separation step, achieving a limit detection of 218 exosomes μL^{-1} in phosphate buffer solution and 10^5 exosomes μL^{-1} in human serum without any previous treatment. This represents a 10-fold gain in sensitivity if compared to conventional ELISA results (10^6 exosomes μL^{-1}). The highest sensitivity was obtained with the CD63 biomarker, meanwhile, CD81 was not affected by the presence of free receptors in serum, thereby allowing the detection of exosomes directly in serum. Later, an electrochemical immunoassay, using amperometry at -0.1 V *vs.* Ag/AgCl using hydroquinone as a mediator, was also investigated, reaching the same limit of the detection value of modified ELISA using the antiCD81 modified magnetic particles. Both methods were able to identify healthy donors and breast cancer patient samples.

In an attempt to address the lack of specificity of some biomarkers, Zhao et al. [146] developed a dual-responsive electrochemistry/fluorescence immunosensor based on a cation-exchange reaction (CER) to determine carcinoembryonic antigen (CEA). The

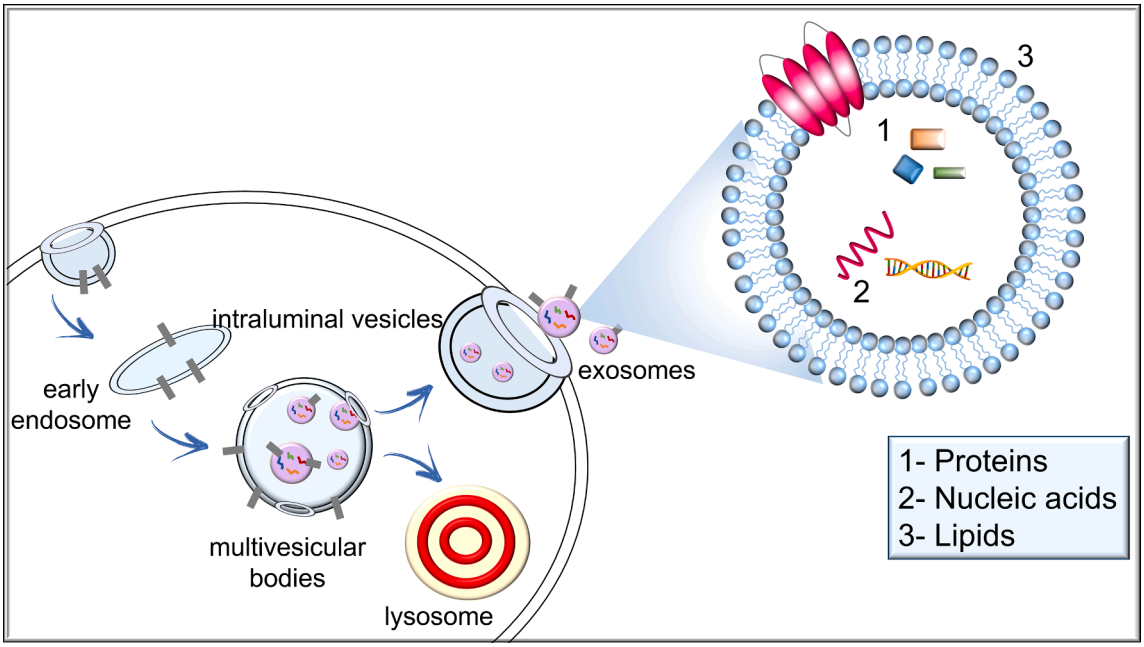

Fig. 4. Illustration of exosomes biogenesis. The early endosome is formed from the cell plasma membrane invagination. Later, multivesicular bodies (MVBs) are generated from endosomal membranes invagination. MVBs can be degraded in the lysosome or released to the intraluminal vesicles known as exosomes by the fusion of MVBs to the plasma membrane mediated by Rab GTPases.. Figure adapted from [140].

hypothesis is that the dual responsive system has a self-correcting ability thereby avoiding false-positive responses because two methods are used to determine the same sample. When consistent results are obtained, the method is shown to be accurate, however in case of discrepancy between the two methods a comparison with a standard method must be provided. This system utilizes CdSe nanoparticles which give a fluorescence response. The electrochemical procedure works by detecting divalent cations, Cd^{2+} released by the addition of Ag^{+} in solution through cation-exchange reaction with the CdSe particles. The Cd^{2+} levels are determined directly through square wave voltammetry (SWV), achieving a detection limit of 1.7 pg mL^{-1}. The fluorescence detection was 10-fold amplified because free Cd^{2+} can trigger the weak fluorescence metal-sensitive dyes (Rhod-5N) and greatly increasing their fluorescence, thereby obtaining a detection limit of 0.25 pg mL^{-1}.

An interesting property of some magnetic nanoparticles is the potential capability of simulating catalytic reactions and/or enzyme mimicking. That becomes desirable since these materials show much greater stability against harsh conditions and also enhances the shelf life of immunoassays [128,147] compared to those containing more fragile species such as enzymes. It is worthy to mention that this property is not limited to magnetite nanoparticles, researchers are also exploring the synthesis of metal oxide (cobalt, zinc, and nickel) nanoparticles with magnetic properties to develop magnetic immunoassays [141, 148–151]. This approach is commonly found as sandwich immunosensors not only for capture and separation of the analyte but also as a mimetic biomarker to facilitate the hydrogen peroxide reduction and thereby allow the quantification of biomarker concentration [152,153]. Faria et al. developed a disposable enzyme-free microfluidic array device (mID) for the detection of CYFRA 21-1 prostate cancer biomarker, in serum samples from healthy and prostate cancer patients, as depicted in Fig. 5. They synthesized $Co_{0.25}Zn_{0.75}Fe_2O_4$ nanoparticles (CoZn--FeONPs) whose magnetic capacity is superior to traditional ferrites (Fe_3O_4), improving the biomolecule separation efficiency and speed, and acting as enzyme mimics, demonstrating peroxidase-like catalysis. Both MNPs presented detection limits of 0.30 and 0.19 fg mL^{-1} for FeONPs and CoZnFeONPs, respectively, which is much lower than the clinical threshold (3.3 ng mL^{-1}) [154]. Table 2 summarizes examples of recently published works on MNP-based electrochemical biosensors.

3.2. Optical immunoassays (SPR)

Surface plasmon resonance (SPR) sensors are based on the changes in the refractive index very close to the sensor surface provoked by binding events between the analyte in solution and the ligand immobilized on the sensor surface [155]. SPR allows label-free real-time monitoring of the molecular interactions, and it is considered an important tool for molecular interaction analysis such as association and dissociation kinetics and ligand-analyte affinity beyond the sensing application. The surface plasmon generation can be achieved by different optical excitation setups, such as the total attenuated reflection (ATR) using prism-coupling, through optical waveguides or diffraction grating (see details in [155,156]). At the most common Kretschmann configuration by the ATR condition [157] (Fig. 6**a**) a thin metal layer (usually Au or Ag) at the base of the prism is interfaced with a dielectric medium (biomolecules layer or solution). At a specific incident angle, named resonance angle (θ_{SPR}), the absorption of light energy by the free oscillating electrons on the metal surface results in an evanescent electromagnetic field, known as surface plasmons, at the metal/dielectric interface [158]. Since SPR conditions are sensitive to small refractive index changes, binding-induced changes can be measured by various modes, such as angular interrogation (the measurement of θ_{SPR} as the minimum reflectivity in an angular scanning), wavelength interrogation (the measurement of the resonance wavelength, λ_{SPR}, as the minimum reflectivity in a wavelength scanning) or by intensity measurement (reflectivity intensity in angular or wavelength interrogation) [155, 158].

Changes in the refractive index depend on the analyte molecular weight and its intrinsically refractive index in such a way that the SPR signal has limited sensitivity for small molecules. Besides that, a direct SPR biosensor can achieve limits of detection at the nM scale but lacks sensitivity for ultra-low concentrations, which is needed for the diagnosis of some diseases. Nanomaterials have been successfully applied for SPR signal amplification as reviewed in [159]. MNPs have gained attention as amplification reagents. The pioneering work looks to be from Teramura et al. [160] who described the signal amplification (100×sensitivity than conventional sandwich-type assay) in angular interrogation sandwich-type assay using MNP-secondary antibody

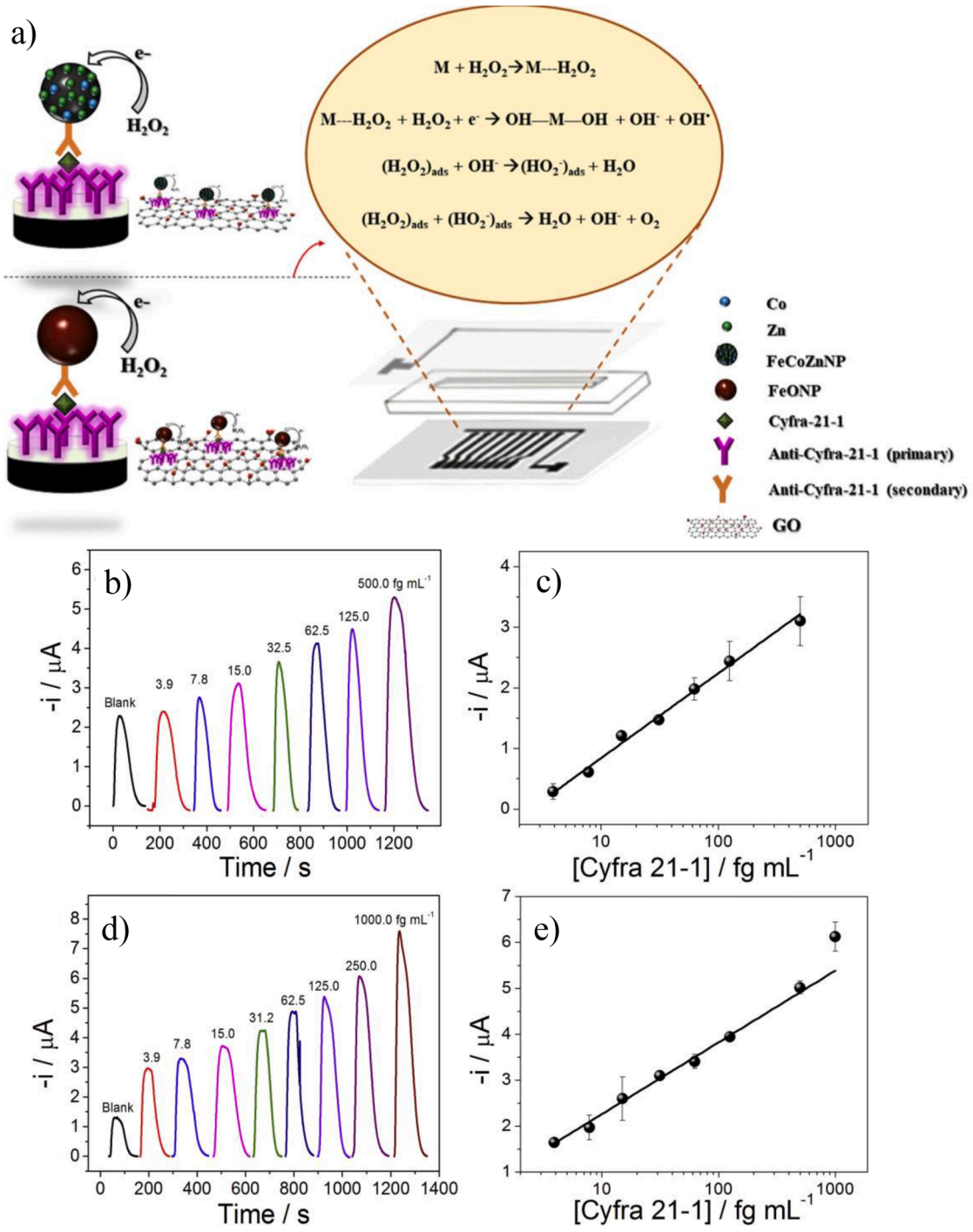

Fig. 5. For the CYFRA 21-1 detection, in the mID, the Ab1 was covalently bound on GO-modified carbon-based electrode (a). The sandwich immunosensor was formed in two steps: first, the biomarker was captured using Ab2-MNP following by the magnetic separation and washing and then the CYFRA-Ab2-MNP bioconjugate was injected in the mID. The pump was stopped, and the CYFRA-Ab2-MNP dispersion was kept for 30 min for the immunoreaction between the biomarker capture on MNPs and Ab1 presented in the electrode surface. Afterward, the pump was restarted to remove the unbounded MNPs by the PBS flow. Finally, the detection solution (50 mmol L^{-1} H_2O_2) was added using the injection valve and the amperometric response was recorded. Amperometric profiles for CYFRA 21-1 in a microfluidic system using 0.01 mol L^{-1} PBS at -0.3 V *vs.* Ag/AgCl, following injection of 50 mmol L^{-1} of H_2O_2 for FeONPs (b) and CoZnFeONPs (d), and corresponding calibration curves for FeONPs (c) and CoZnFeONPs (e). Reproduced with permission from [154].

conjugates. A schematic representation comparing the direct and sandwich-assay using MNP-secondary antibody conjugates are depicted in Fig. 6**b** and **c**, respectively. Fig. 6**d** and **e** represent the reflectivity plot and the SPR sensorgram (signal in function of time) of the respective direct and amplified assays.

In 2007, Sun et al. [161] reported the signal amplification using MNP in SPR direct assays. The sensor was functionalized with MNP-coupled antibodies instead of the sole antibody. Despite the easy immobilization of the antibodies to the sensing surface by the action of an external magnetic field, the sensitivity of the wavelength modulation SPR sensor was enhanced by shifting the resonance wavelength towards a longer wavelength. Since that, several works have been published concerning the application of MNP in SPR sensing in different approaches including core-shell nanocomposites with Au and Ag nanoparticles [162–165],

Table 2
Summary of some recently published works on MNP-based electrochemical biosensors.

Platform	Analyte	MNP role	Interrogation method	Range of detection	Limit of detection	Ref.
Magnetic bead/antibody/AuNPs immobilised on carbon electrodes	Salmonella	Binding of target and concentration at electrode	Differential pulse voltammetry	100-700 cells ml^{-1}	100 cells ml^{-1}	[134]
Superparamagnetic particle/antibody on carbon electrodes in microfluidic cell	Estrogen receptor alpha	Binding of target/HRP, concentration at electrode	Amperometry	16.6-513 fg ml^{-1}	10 fg ml^{-1}	[135]
Streptavidin modified magnetic beads immobilized on screen-printed electrodes	PSA	Binding of target and concentration at the electrode	Amperometry	5-100 ng ml^{-1}	1.86 ng ml^{-1}	[136]
Antibody modified magnetic beads immobilized on AuNP electrodes	PSA	Binding of target and concentration at the electrode	Rotating disc amperometry	0-40 ng ml^{-1}	0.5 pg ml^{-1}	[138]
Streptavidin-magnetic beads modified with enzyme and antibody on AuNP electrodes	IL-6, IL-8	Binding of target/HRP, the concentration at the electrode	Amperometry	IL-6 0-5000 fg ml^{-1} IL-8 0-3750 fg ml^{-1}	IL-6 5 fg ml^{-1} IL-8 7 fg ml^{-1}	[139]
Antibody modified magnetic beads on magnetic electrodes	Breast cancer exosomes	Binding of target and concentration at the electrode	Amperometry	antiCD81 10^2-10^6 exosomes ul^{-1} in serum	10^5 exosomes ul^{-1}	[143]
Antibody modified magnetic beads on magnetic electrodes	Breast cancer exosomes	Binding of target and concentration at electrode	Amperometry	antiCD24/CD340 2×10^4-2×10^7 exosomes ul^{-1} in serum	antiCD24 1.94×10^5 antiCD340 1.02×10^6 exosomes ul^{-1}	[145]
Magnetic bead/antibody/CNT/CdSe on GCE	Carcino Embryonic Antigen	Binding of target and concentration at the electrode	Square wave voltammetry Fluorescence	SWV 5 pg ml^{-1}-50 ng ml^{-1} Fluor 1 pg ml^{-1}-20 ng ml^{-1}	SWV 1.7 pg ml^{-1} Fluor 0.25 pg ml^{-1}	[146]
Antibody modified Fe_3O_4 core-shell particles on GCE	PSA	Electrode modification and target binding	Differential pulse voltammetry	1 pg ml^{-1}-100 ng ml^{-1}	0.45 pg ml^{-1}	[149]
Antibody modified Fe_3O_4 particles on graphene oxide	PSA	Binding of target and catalytic effect	Amperometry	61 fg ml^{-1}-3.9 pg ml^{-1} or 9.8-624 pg ml^{-1}	15 fg ml^{-1} or 4.9 pg ml^{-1}	[152]
Superparamagnetic particle/antibody on carbon electrodes in microfluidic cell	PSA, IL-6	Binding of target/HRP, concentration at electrode	Amperometry	PSA 0.225-20 pg ml^{-1} IL-6 0.3-15 pg ml^{-1}	PSA 0.23 pg ml^{-1} IL-6 0.30 pg ml^{-1}	[153]
Antibody modified $Co_{0.25}Zn_{0.75}Fe_2O_4$ particles on carbon electrode	CYFRA 21-1	Binding of target and catalytic effect	Amperometry	3.9-1000 fg ml^{-1}	0.19 fg ml^{-1}	[154]

*IL = Interleukin, PSA = Prostate specific antigen

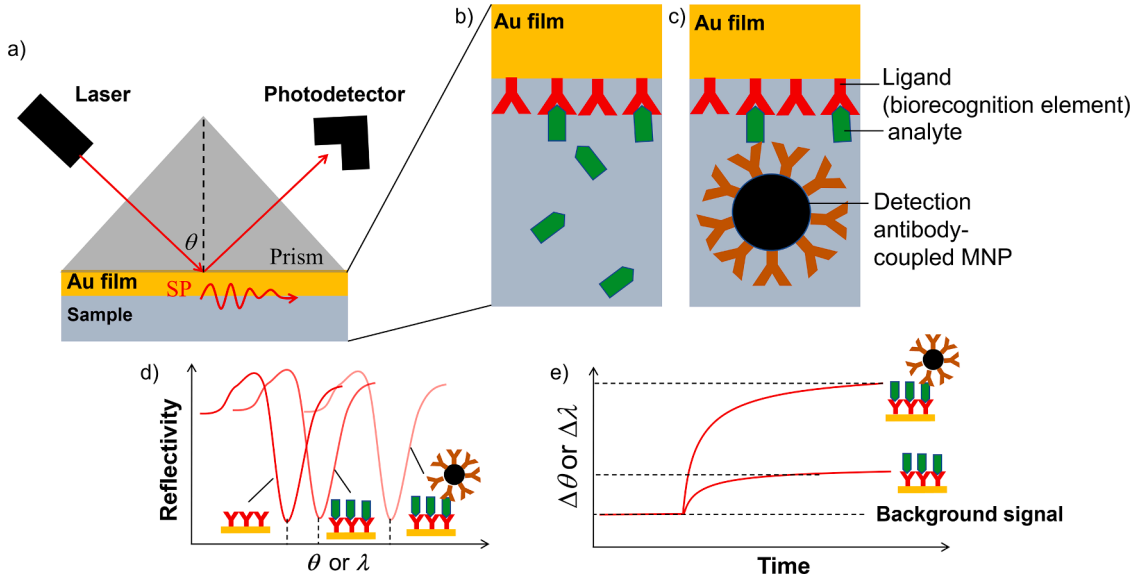

Fig. 6. Schematic of the prism-coupling Kretschmann configuration (a). θ: incident angle. Representation of the direct-immunoassay (b) and sandwich-assay by MNP-coupled detection antibody (c). Comparison between the SPR response for direct and MNP-based sandwich-assay: reflectivity measurement (d) and real-time monitoring of the SPR response (e) by angular (Δθ) or wavelength interrogation (Δλ).

surface plasmon-enhanced epifluorescence detection [166], among others. A summary of the recent works concerning the MNP use in SPR sensors is presented in Table 3.

Besides the signal amplification, MNPs exhibit unique magnetic properties to allow the analyte capture, purification, and concentration from complex matrixes. As the body fluids (*e.g.* plasma, urine, and stool)

Table 3
Summary of the recently published works on MNP-based SPR biosensors.

Architecture [reference]	Analyte	SPR Mode*/ interrogation	MNP role	Achievement compared to traditional SPR	Limit and range of detection
Sandwich assay: Fe_3O_4@ Au nanoparticles functionalized with Apt2. Sensor surface-functionalized with Apt1 [162]	thrombin	Angular interrogation	Signal amplification	SPR angle shift enlarged 5 times compared to the control group without the nanoparticles (at 100 nM)	0.6 nM (0.1 – 100 nM)
Sandwich-assay: Fe_3O_4 MNP functionalized with capture Ab. Sensor surface-functionalized with detection Ab [176]	*Salmonella enteritidis*	Angular interrogation	Preconcentration, signal amplification	4 orders of magnitude improvement in sensitivity compared to the direct SPR	Lower than 14 CFU (1.4×10^4 – 1.4×10^9 CFU mL^{-1})
Sandwich-assay: Fe_3O_4@ Au nanoparticles functionalized with Ab2 for sandwich-assay. Sensor surface-functionalized with Ab1 [181]	CFP-10 (tuberculosis)	Angular interrogation	Signal amplification	The limit of detection by direct detection was 0.1 μg mL^{-1}	0.1 ng mL^{-1} (0.1 – 100 ng mL^{-1})
Sandwich-assay: commercial MNP linked to the EVs. Au sensor functionalized with anti-CD81 [171]	Extracellular vesicles (EVs)	Grating-coupled/ wavelength interrogation	Preconcentration, overcomes slow-diffusion-limited mass transfer, signal amplification	No response by direct SPR assay in the same range	0.76 μg mL^{-1} (0.76 – 3.0 μg mL^{-1})
Indirect competition assay: mAb-MNP incubated with different concentrations of E_2 and injected through the Au sensor modified with E_2-BSA [183]	Estradiol (E_2)	Angular interrogation	Signal amplification	The lower limit of detection and wider range than without MNP (with a limit of 3.24 ng mL^{-1} and range of 3.906−1000 ng mL^{-1})	0.814 ng mL^{-1} (1.953−2000 ng mL^{-1})
Combined direct SPR and plasmonically enhanced fluorescence (PEF) readout: EV analyte was first bound to MNP via lipid-binding protein CTB with biotin tags [166]	Extracellular vesicles (EVs)	Grating-coupled/ wavelength interrogation	Preconcentration, overcomes slow-diffusion-limited mass transfer, signal amplification	Combined SPR and fluorescence detection. 2-fold signal improvement for the propagating surface polaritons coupling with the fluorophores in PEF measurements and signal-to-noise ratio 2.4-fold higher with the SPR assay than PEF	-
Sandwich-assay: polydopamine-Ag@Fe_3O_4/reduced graphene oxide bind to Ab2. Gold sensor surface-functionalized with hollow gold nanospheres (HGNPs) and anti-rabbit IgG (Ab_1) [179]	Rabbit IgG	wavelength interrogation	Signal amplification	The lowest concentration detected was 132 times lower than the MPA-based gold sensor	0.019 μg mL^{-1}

*ATR prism-coupled SPR otherwise mentioned.

are a complex mixture of proteins, lipids, and many other components that can both hamper the analyte association to the surface or bind nonspecifically to the sensing surface. These steps are especially important to detect ultralow concentrations, in which the background signal from the matrix can hamper a lower limit of detections. In 2009, Soelberg et al. [167] described the detection of pg level of *Staphylococcal enterotoxin B* (SEB) from stool samples using MNP-conjugated anti-SEB. Incubation steps followed by four washing steps were performed using a permanent magnet to allow sequential elution and washing of residues. The MNP-anti-SEB-analyte conjugates were isolated by the permanent magnet, eluted in PBS, and run through the capture Ab-functionalized sensing surface [168].

Before citing the advantages of using MNP in SPR platforms in detail, some drawbacks may be raised. Compared to the gold nanoparticles (AuNP), the surface chemistry of the MNP does not allow the direct biomolecules anchoring, which has been solved with shells of Au [169, 170] or by using streptavidin-biotin interaction [160,171]. Additionally, special attention should be given to the stability of the nanoparticles once they tend to easily agglomerate. Despite these few difficulties, the benefits of using MNP in SPR sensing platforms are summarized as:

(i) external magnetic field-induced sensor functionalization or analyte attraction;
(ii) signal amplification in sandwich-type assays;
(iii) purification and enrichment from complex matrixes (decreased background signal);
(iv) other advantages as low-cost, easy synthesis, and commercial availability of biologically modified-MNP.

3.2.1. *External magnetic field-induced protein immobilization or analyte attraction for direct assays*

Molecules coupled to MNP can be rapidly attracted to the sensing surface by using a permanent magnet placed behind the sensing surface. Although it is easier to approach the permanent magnet in grating-coupled SPR platforms (flat surface, no need of prism) [166,172,173], magnetic pillars have been successfully used by placing them under the prism in Kretschmann configuration [163,165,169]. MNPs have been used to achieve effective and fast immobilization of the capture antibody on the sensing surface in direct SPR assays. In this setup, antibodies are conjugated to the MNP and further flowed to the channel under the action of a magnetic pillar [161,169,170]. These direct assays are especially interesting in MNP-AuNP nanocomposites because while the MNP provides the magnetic-driven carrier, AuNP confers enhanced sensitivity because they have their surface plasmons due to the collective oscillation of their conduction electrons (localized surface plasmon resonance - LSPR). The coupling of the localized surface plasmons and the propagating surface plasmons provides an amplified SPR signal [174,175]. This also leads to the resonant wavelength moving to a longer wavelength resulting in an enhancement of the sensitivity in wavelength interrogation SPR [156]. The Au shell also provides an easy protocol for antibody anchoring by the well-established thiol-functionalization followed by NHS:EDC chemistry [170]. Filipczak et al. [163] immobilized MNP/Ag/Au nanocomposites on the sensing surface achieving a redshift of the resonant wavelength (improved sensitivity). The nanocomposite conjugated with anti-dog IgG allowed detection of dog IgG from 0.15 to 40.00 μg mL^{-1}, while the control sensor was based on the thiol-functionalization with MPA/antibody sensor, responded from 1.25 to 20 μg mL^{-1}, with a limit of quantification about 8 times lower using the nanocomposite based sensor. Another advantage of

using magnetic force-driven immobilizing of antibodies is related to the reuse of the sensors, which is quite costly. After switching off the magnetic field, washing and flushing steps with water or buffer can effectively remove the MNP-antibody composites from the sensor surface [161,169,170] for further introduction of new conjugates.

Besides the antibody immobilization, MNPs were used as "vehicles" for the rapid delivery of the target β human chorionic gonadotropin (βhCG) from the sample to the sensor surface [173]. MNPs were conjugated to the detection antibody (dAb) and further incubated with βhCG (analyte). The complex MNP-dAb-βhCG was flowed through the capture antibody functionalized Au sensor with an applied magnetic field gradient (0.10 T mm^{-1}). After switching off the magnetic field and proper washing, the sensor response was determined. The speed of the MNP-dAb-βhCG under magnetic field was calculated to be 6×10^{-2} mm s^{-2}, which is 13- and 180-fold faster than the diffusion rates of hCG and MNP (of 4.8×10^{-3} and 3.3×10^{-4} mm s^{-1}), respectively. Furthermore, an improved sensitivity by 4 orders of magnitude compared to direct SPR was achieved, with a limit of detection below pM [173].

Reiner et al. [171] demonstrated a grating-coupled SPR system for extracellular vesicles (EVs) detection. The analyte was pre-concentrated by binding to MNP via lipid-binding proteins (Fig. 7**a**-1). The EV-MNP conjugate interacts with the antibody (anti-CD81) functionalized to the gold surface (**2**) allowing the detection by the optical system based on grating-coupled SPR (**3**). The presented setup combined an increased mass transfer rate and amplified refractive index changes. The sensor assembly was demonstrated by the sensorgram in Fig. 7**b** with the difference in SPR wavelength ($\delta\lambda_{SPR}$) before and after the anti-CD81 immobilization and proper washing and blocking of non-specific sites.

A negative control composed of MNP without EVs was run to demonstrate the specific response to the EVs. The sensorgram in Fig. 7**c** shows that after injection of the control sample of MNP under magnetic field action, the SPR signal decreases (between t1 e t2) with the MNP attraction to the sensor surface. After removing the magnetic field, the λ_{SPR} returns gradually to the baseline value. This is related to the strong light absorption from the MNPs and can be verified as a broader and tilted SPR dip in the reflectivity curves in Fig. 7**d** when MNP are immobilized, in t2, t4, and t5). When the EV-MNP sample was run, a permanent $\delta\lambda_{SPR}$ was verified even after removing the magnetic field [171].

3.2.2. *Signal amplification in sandwich-type assays*

Signal reagent amplification based on secondary antibody-nanoparticles conjugates has demonstrated successful results in ultrasensitive SPR sensing due to the increased refractive index change caused by the mass increase at the interface. High mass and refractive index iron oxides MNP have been applied as amplifying reagent in SPR sandwich-assays for bacteria detection [168,172,176], tumor markers [164,177], hormones [160,173], proteases [162,178] and immunoglobulins [179].

Sandwich-assays based on MNPs amplification is based on the attachment of secondary antibodies to the heavy MNP. The conjugation of the secondary antibodies to the MNP surface is not-so-well established as-is for AuNPs. Different strategies can be used to anchor the detection proteins to the MNP surface, including biotin-labeled secondary antibody and streptavidin-conjugated MNP [160]. An additional shell of Au for easy thiol-functionalization by EDC:NHS chemistry [169,170], the

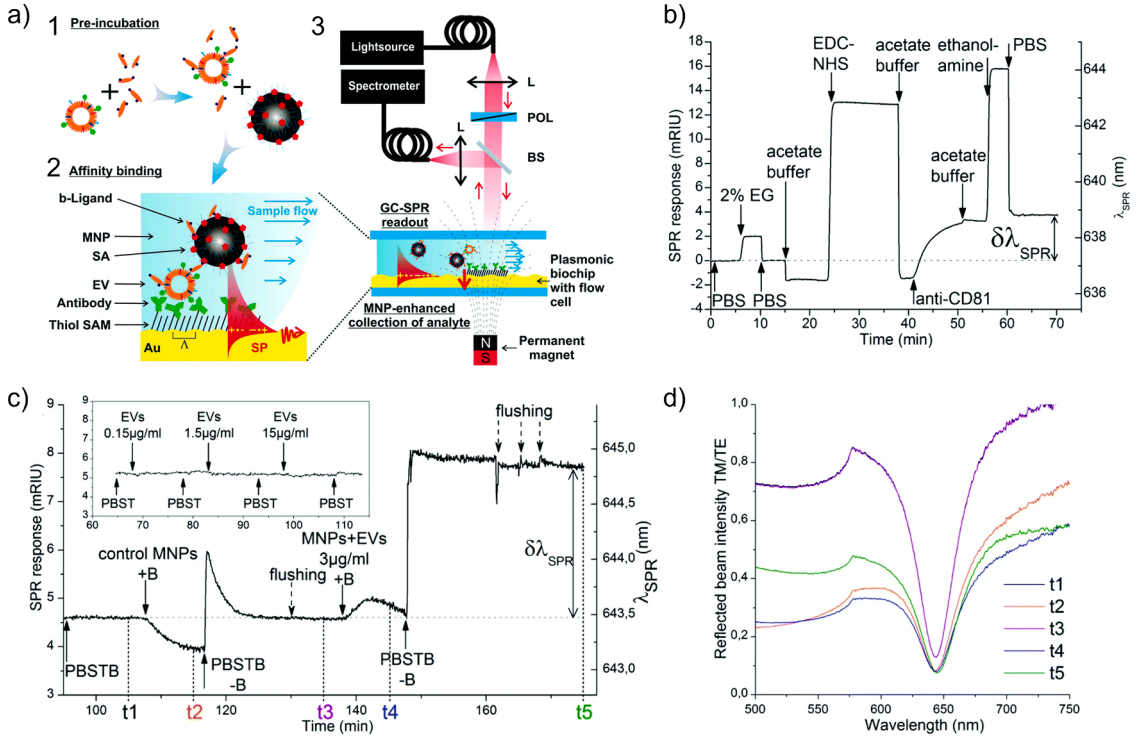

Fig. 7. (a) Schematic of the grating-coupled SPR sensor system and assay. (1) pre-incubation of the extracellular vesicles (EV) with the biotinylated lipid-binding ligand (b-ligand) and streptavidin (SA) coated magnetic nanoparticles (MNP). (2 Surface chemistry on the gold sensor for affinity binding of the target. (3) Optical setup of the MNP-enhanced SPR assay and the system allowing the pulling of the target analyte to the sensor surface. SAM: self-assembled monolayer, SP: surface plasmon, L: lens, POL: polarizer, BS: beam splitter, GC-SPR: grating-coupled surface plasmon resonance. (b) SPR sensorgram for the gold sensor functionalization with anti-CD81. EG: ethyleneglycol, PBS: phosphate buffered saline, EDC: N-(3-dimethylaminopropyl)-N'-ethylcarbodiimide, NHS: N-hydroxysuccinimide. (c) SPR sensorgram using anti-CD81 functionalized Au sensor with the injection of negative control (MNP without EVs) under a magnetic field gradient (+B), after incubation of 10 min the magnetic field was removed (-B), the surface was washed by flushing. Then, sample (MNP+EV) was injected under a magnetic field (+B), incubated for 10 min, magnetic field was removed for washing. $\delta\lambda_{SPR}$: SPR response change caused by MNP-bound EVs binding to the surface; mRIU: mili refractive index units, PBST or PBSTB: phosphate buffered saline with Tween 20 or Tween 20 and bovine serum albumin. (d) Wavelength reflectivity spectra from different time-points indicated in the sensorgram. Reproduced with permission from [171].

shell of SiO_2 for further 3-aminopropyltrimethoxysilane (APTMS) modification [165] and copper-catalyzed alkyne-azide cycloaddition [180].

Li et al. [179] used a hollow gold nanoparticle (HGNPs)-modified gold sensor to anchor the capture antibody (Ab_1) thus inducing electromagnetic coupling between the HGNPs and the gold surface. After interaction with different concentrations of IgG sample, a conjugate formed by the detection antibody (Ab_2) with polydopamine deposited on the core-shell structure of the silver-Fe_3O_4 was distributed to the reduced-graphene oxide (PDA-Ag@Fe_3O_4/rGO), then used for detection and amplification. The Ab_2-PDA-Ag@Fe_3O_4/rGO conjugate is easily prepared since the magnetic field was used for isolation and washing protocols. A limit of detection of 0.019 μg mL^{-1} was achieved, which is 132 and 16 times less than those obtained with conventional direct SPR and Au-HGNPs (without the sandwich approach), respectively.

Zou et al. [181] developed a sensor for tuberculosis using magneto-plasmonic nanoparticles (MPNs) with three different morphologies (sphere, short spiky, and long spiky) of Fe_3O_4@AuNPs composites. The sandwich SPR immunoassay was constructed by the immobilization of anti-CFP-10 (Ab1) onto the Au sensor chip via Au-S bonds. After incubation with the target protein CFP-10, the MPNs-Ab2 conjugate was flowing to signal amplification (schematic in Fig. 8**a**). Fig. 8**b** depicts the SPR angle shift due to the Ab1 immobilization onto the gold chip and proper washing and blocking. Comparing the three different shapes (Fig. 8**c**), the spherical MPNs demonstrated the best performance in signal amplification. Fig. 8**d** depicts the sensorgrams for the detection of CFP-10 between 0.1–100 ng mL^{-1}. The limit of detection was 0.1 ng mL^{-1}. In the same concentration range, the detection was impossible without the MNP-based sandwich assay [181].

3.2.3. *Signal amplification by decreasing the background signal*

Overcoming the interference from complex matrixes as a serum, saliva, and stool is important to reduce the background signal and so achieve low limits of detection as demanded diagnosis of many important analytes. Many compounds in these complex samples can impede the binding of the analyte to the SPR sensor as well bind nonspecifically to the surface, interfering with the signal [168]. MNPs have been applied for magnetic-assisted separation of many biological analytes such as cells, nucleic acids, and proteins [121,182]. Usually, the magnetic separation is performed by adding MNP functionalized with affinity ligands towards the target directly to the sample, and after an incubation time, the target molecules or cells are bound to the MNP forming stable magnetic complexes. Non-desired compounds can be washed and removed from the solution while a magnetic separator (permanent magnet) is used to separate the magnetic complex [182]. For the SPR measurements, the MNP-target complex can be directly flowed to the sensor surface properly functionalized, for example, with a capture antibody [168,176]. Indeed, MNP can provide both easy analyte separation and signal amplification in sandwich-type SPR immunosensors.

Liu et al. [176] demonstrated that antibody-functionalized Fe_3O_4 MNPs (immunoMNPs) can selectively recognize and isolate *Salmonella enteritidis* from a sample matrix. The immunoMNPs were incubated with samples containing bacteria in a 37 °C water bath for 40 min. After the *S. enteritidis* capture by the immunoMNP, the separation was performed using a magnet. After redispersion in PBS, the *S. enteritidis*-immunoMNPs suspension has directly flowed over the SPR sensor chip functionalized with the PAb (polyclonal anti-*Salmonella* antibody). *S. enteritidis* was detected at concentrations as low as 14 CFU/mL with a linear relationship between 1.4×10^1–1.4×10^9 CFU/mL. The sensitivity was improved 4 orders of magnitude compared to the regular SPR. A test performed in eggshell demonstrated recovery

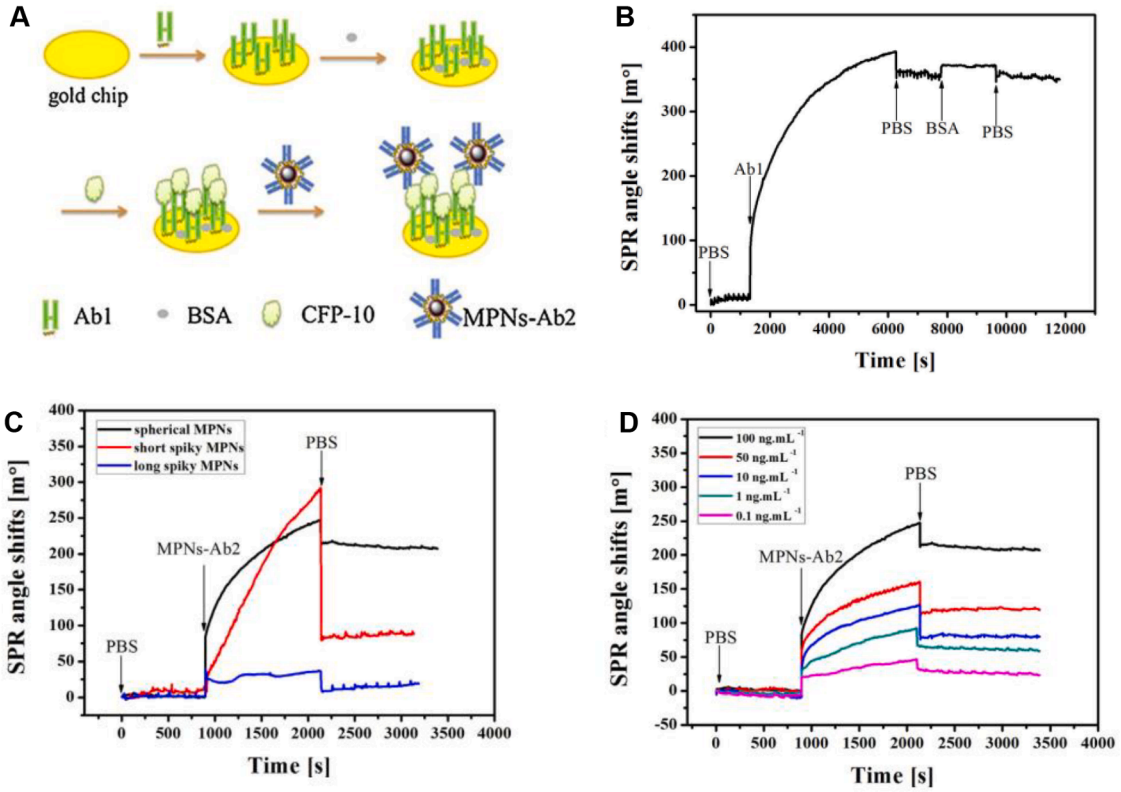

Fig. 8. (a) Schematic of the sandwich-SPR immunoassay for the CFP-10 detection. Ab1: Capture antibody, BSA: bovine serum albumin (blocking reagent), CFP-10: specific antigen (target), MPNs-Ab2: magneto-plasmonic nanoparticles-detection antibody conjugate. (b) SPR sensorgram of the sensor fabrication. PBS: phosphate-buffered saline. (c) SPR sensorgram showing the signal amplification with the spherical, short spiky, and long spiky shaped nanoparticles at CFP-10 concentration of 100 ng mL^{-1}. (d) SPR sensorgram showing the amplification with spherical MPN to various concentrations of CFP-10. Reproduced with permission from [181].

of 92.76–113.25% [176].

4. Conclusion

In recent years there has been a large increase in the research and development on magnetic nanoparticles for biomedical applications. The ability to control particle size, shape, and surface functionality of the NPs has led to a widespread investigation into potential uses. Magnetic nanoparticles also have the advantages that they can be used in applications such as hyperthermia treatment and can also be specifically targeted to a specific location within the body by an alternating magnetic field. MNPs have a high surface area to volume ratio that allows high levels of substitution making them ideal for drug delivery, and their ability to be incorporated into composites such as magnetic hydrogels or liposomes increases their biocompatibility and potential medical applications.

One potentially great benefit for MNPs is that they could be highly suitable for a combined attack on diseases such as cancer, where the MNP could be used as a combined hyperthermal and drug delivery agent rather than two separate treatments. One can envisage a treatment where magnetic fields are used to locate funtionalized MNPs into a tumor, magnetic hyperthermia used to destroy the tumor, and then therapeutic drugs released by the MNPs to treat any remaining traces.

Some issues remain to be solved with these systems. Firstly the size and shape of these MNPs will have great effects on their efficiencies, and suitable synthetic procedures need to be developed, and the resultant materials studied to determine optimal behavior. Aggregation of MNPs is also an issue since it can affect their efficiency and potential toxicity. Toxicity studies will need to be addressed, although the iron oxide nanoparticles are thought to be much less toxic than many other nanoparticle types proposed for biomedical applications.

Although much work on magnetic hyperthermia and drug delivery using MNPs have been carried out in animal models, translating this into suitable treatments for human patients remains the major challenge. Assessments have to be made of the effects of MNP size, shape, substitution, and dosage before they can be widely applied. Toxicity issues need to be addressed and resolved. Initial applications of MNPs in hyperthermia and drug delivery treatments have been successful in the laboratory, but before clinical use, wide *in vitro* and *in vivo* trials combined with toxicity and long-term MNP stability tests need to be carried out. Mathematical modeling may also prove to be of use in addressing these issues.

However, so far, MNPs have demonstrated their ability to be synthesized and functionalized almost to order, and a large number of proof of concept trials determined their potential as a new species of effective therapeutic agents for many debilitating and life-threatening illnesses. It seems almost inevitable that we will see these types of treatment becoming much more common in the future.

Concerning biosensors, they have shown to be excellent in sample treatment, due to that can separate the analyte from complex samples (urine and blood) and pre-concentrate it on the surface of the electrode, increase signal and selectivity. One of the biggest challenges is to find the appropriate size, shape, and coating to make it biocompatible, stable, and successfully adhere to biomolecules of interest. Also, the coating plays an essential role in various applications: being highly biocompatible and stable, it would allow the adhered biomolecules to remain active for longer within the body and satisfactorily controlling their release or remaining attached for long periods to be stored and used for diagnosis. Another essential advantage of magnetic nanoparticles is that they can be used for the detection of cancer. The magnetic nanoparticles are coated with antibodies targeting cancer cells or cancer-associated biomolecules; this can be used as biosensors. For example, a blood sample can be injected onto a microfluidic chip, including magnetic nanoparticles in it. These modified magnetic nanoparticles react with the analyte of interest, giving an analytical response, and the remainder of the blood sample flows freely in the microfluidic systems [184]. FDA-approved applications of iron oxide nanoparticles include cancer diagnosis, cancer hyperthermia therapy, and iron deficiency anemia [185]. Additionally, magnetic nanoparticles have been proposed as such a tool against the fight against COVID-19 [186,187], and they have been explored to remove pathogens or viral particles from contaminated water, blood plasma, or others sources [188–190].

Declaration of Competing Interest

The authors declare that they have no known competing financial interests or personal relationships that could have appeared to influence the work reported in this paper.

Acknowledgments

The authors are thankful for the financial assistance from the Brazilian funding agencies: São Paulo Research Foundation - FAPESP (2014/23546-1, 2016/00991-5, 2018/22214-6) and the National Council for scientific and technological development – CNPq.

References

[1] R.K. Gilchrist, R. Medal, W.D. Shorey, R.C. Hanselman, J.C. Parrott, C.B. Taylor, Selective inductive heating of lymph nodes, Ann. Surg. 146 (1957) 596–606, https://doi.org/10.1097/00000658-195710000-00007.
[2] H. Vaghari, H. Jafarizadeh-Malmiri, M. Mohammadlou, A. Berenjian, N. Anarjan, N. Jafari, S. Nasiri, Application of magnetic nanoparticles in smart enzyme immobilization, Biotechnol. Lett. 38 (2016) 223–233, https://doi.org/10.1007/s10529-015-1977-z.
[3] N. Malhotra, J.S. Lee, R.A.D. Liman, J.M.S. Ruallo, O.B. Villaflores, T.R. Ger, C. D. Hsiao, Potential toxicity of iron oxide magnetic nanoparticles: a review, Molecules 25 (2020) 3159, https://doi.org/10.3390/molecules25143159.
[4] J. Kolosnjaj-Tabi, L. Lartigue, Y. Javed, N. Luciani, T. Pellegrino, C. Wilhelm, D. Alloyeau, F. Gazeau, Biotransformations of magnetic nanoparticles in the body, Nano Today 11 (2016) 280–284, https://doi.org/10.1016/j.nantod.2015.10.001.
[5] A. Rivera-Rodriguez, C.M. Rinaldi-Ramos, Emerging biomedical applications based on the response of magnetic nanoparticles to time-varying magnetic fields, Annu. Rev. Chem. Biomol. Eng. 12 (2021) 163–185, https://doi.org/10.1146/annurev-chembioeng-102720-015630.
[6] M. Monteserín, S. Larumbe, A.V. Martínez, S. Burgui, L. Francisco Martín, Recent advances in the development of magnetic nanoparticles for biomedical applications, J. Nanosci. Nanotechnol. 21 (2021) 2705–2741, https://doi.org/10.1166/jnn.2021.19062.
[7] K. Parekh, J. Nair, A. Bhardwaj, Biosynthesis of magnetite nanoparticles: an eco-friendly and scalable approach, Adv. Nat. Sci. Nanosci. Nanotechnol. 11 (2020), 035014, https://doi.org/10.1088/2043-6254/aba896.
[8] A. Bahadur, A. Saeed, M. Shoaib, S. Iqbal, M.I. Bashir, M. Waqas, M.N. Hussain, N. Abbas, Eco-friendly synthesis of magnetite (Fe_3O_4) nanoparticles with tunable size: Dielectric, magnetic, thermal and optical studies, Mater. Chem. Phys. 198 (2017) 229–235, https://doi.org/10.1016/j.matchemphys.2017.05.061.
[9] P. Tartaj, M. del Puerto Morales, S. Veintemillas-Verdaguer, T. González-Carreño, C.J. Serna, The preparation of magnetic nanoparticles for applications in biomedicine, J. Phys. D. Appl. Phys. 36 (2003) R182–R197, https://doi.org/10.1088/0022-3727/36/13/202.
[10] A.H. Lu, E.L. Salabas, F. Schüth, Magnetic nanoparticles: synthesis, protection, functionalization, and application, Angew. Chem. Int. Ed. 46 (2007) 1222–1244, https://doi.org/10.1002/anie.200602866.
[11] L. Mohammed, H.G. Gomaa, D. Ragab, J. Zhu, Magnetic nanoparticles for environmental and biomedical applications: a review, Particuology 30 (2017) 1–14, https://doi.org/10.1016/j.partic.2016.06.001.
[12] A.R. Iliasov, T.R. Nizamov, V.A. Naumenko, A.S. Garanina, S.S. Vodopyanov, A. A. Nikitin, A.G. Pershina, A.A. Chernysheva, Y. Kan, P.S. Mogilnikov, O. N. Metelkina, I.V. Schetinin, A.G. Savchenko, A.G. Majouga, M.A. Abakumov, Non-magnetic shell coating of magnetic nanoparticles as key factor of toxicity for cancer cells in a low frequency alternating magnetic field, Colloids Surf. B Biointerfaces 206 (2021), 111931, https://doi.org/10.1016/j.colsurfb.2021.111931.
[13] D.W. Wong, W.L. Gan, Y.K. Teo, W.S. Lew, Interplay of cell death signaling pathways mediated by alternating magnetic field gradient, Cell Death Discov. 4 (2018) 49, https://doi.org/10.1038/s41420-018-0052-7.
[14] N. Hoshyar, S. Gray, H. Han, G. Bao, The effect of nanoparticle size on *in vivo* pharmacokinetics and cellular interaction, Nanomedicine 11 (2016) 673–692, https://doi.org/10.2217/nnm.16.5.
[15] X. Li, B. Wang, S. Zhou, W. Chen, H. Chen, S. Liang, L. Zheng, H. Yu, R. Chu, M. Wang, Z. Chai, W. Feng, Surface chemistry governs the sub-organ transfer, clearance and toxicity of functional gold nanoparticles in the liver and kidney, J. Nanobiotechnol. 18 (2020) 45, https://doi.org/10.1186/s12951-020-00599-1.

[16] C. Janko, T. Ratschker, K. Nguyen, L. Zschiesche, R. Tietze, S. Lyer, C. Alexiou, Functionalized superparamagnetic iron oxide nanoparticles (SPIONs) as platform for the targeted multimodal tumor therapy, Front. Oncol. 9 (2019) 1–9, https://doi.org/10.3389/fonc.2019.00059.
[17] K. Mylkie, P. Nowak, P. Rybczynski, M. Ziegler-Borowska, Polymer-coated magnetite nanoparticles for protein immobilization, Materials 14 (2021) 248, https://doi.org/10.3390/ma14020248 (Basel).
[18] M. Bilal, Y. Zhao, T. Rasheed, H.M.N. Iqbal, Magnetic nanoparticles as versatile carriers for enzymes immobilization: a review, Int. J. Biol. Macromol. 120 (2018) 2530–2544, https://doi.org/10.1016/j.ijbiomac.2018.09.025.
[19] S.D. Soelberg, R.C. Stevens, A.P. Limaye, C.E. Furlong, Surface plasmon resonance detection using antibody-linked magnetic nanoparticles for analyte capture, purification, concentration, and signal amplification, Anal. Chem. 81 (2009) 2357–2363, https://doi.org/10.1021/ac900007c.
[20] Z.P. Aguilar, Targeted drug delivery, Nanomaterials for Medical Applications (2013) 181–234, https://doi.org/10.1016/B978-0-12-385089-8.00005-4.
[21] M. Fathi, S. Majidi, P.S. Zangabad, J. Barar, H. Erfan-Niya, Y. Omidi, Chitosan-based multifunctional nanomedicines and theranostics for targeted therapy of cancer, Med. Res. Rev. 38 (2018) 2110–2136, https://doi.org/10.1002/med.21506.
[22] R. Sawisai, R. Wanchanthuek, W. Radchatawedchakoon, U. Sakee, Simple continuous flow synthesis of linoleic and palmitic acid-coated magnetite nanoparticles, Surf. Interfaces. 17 (2019) 100344. 10.1016/j.surfin.2019.100344.
[23] J. Gao, H. Gu, B. Xu, Multifunctional magnetic nanoparticles: design, synthesis, and biomedical applications, Acc. Chem. Res. 42 (2009) 1097–1107, https://doi.org/10.1021/ar9000026.
[24] D. Wilson, E.M. Materón, G. Ibáñez-Redín, R.C. Faria, D.S. Correa, O.N. Oliveira, Electrical detection of pathogenic bacteria in food samples using information visualization methods with a sensor based on magnetic nanoparticles functionalized with antimicrobial peptides, Talanta 194 (2019) 611–618, https://doi.org/10.1016/j.talanta.2018.10.089.
[25] T.N. Le, T.D. Tran, M. Il Kim, A convenient colorimetric bacteria detection method utilizing chitosan-coated magnetic nanoparticles, Nanomaterials 10 (2020) 92, https://doi.org/10.3390/nano10010092.
[26] C. Xu, O.U. Akakuru, J. Zheng, A. Wu, Applications of iron oxide-based magnetic nanoparticles in the diagnosis and treatment of bacterial infections, Front. Bioeng. Biotechnol. 7 (2019) 1–15, https://doi.org/10.3389/fbioe.2019.00141.
[27] K. Deligkaris, T.S. Tadele, W. Olthuis, A. van den Berg, Hydrogel-based devices for biomedical applications, Sens. Actuators B Chem. 147 (2010) 765–774, https://doi.org/10.1016/j.snb.2010.03.083.
[28] A.K. Gupta, R.R. Naregalkar, V.D. Vaidya, M. Gupta, Recent advances on surface engineering of magnetic iron oxide nanoparticles and their biomedical applications, Nanomedicine 2 (2007) 23–39, https://doi.org/10.2217/17435889.2.1.23.
[29] V.F. Cardoso, A. Francesko, C. Ribeiro, M. Bañobre-López, P. Martins, S. Lanceros-Mendez, Advances in magnetic nanoparticles for biomedical applications, Adv. Healthc. Mater. 7 (2018), 1700845, https://doi.org/10.1002/adhm.201700845.
[30] M. Freitas, H.P.A. Nouws, E. Keating, C. Delerue-Matos, High-performance electrochemical immunomagnetic assay for breast cancer analysis, Sens. Actuators B Chem. 308 (2020), 127667, https://doi.org/10.1016/j.snb.2020.127667.
[31] C.S.S.R. Kumar, F. Mohammad, Magnetic nanomaterials for hyperthermia-based therapy and controlled drug delivery, Adv. Drug Deliv. Rev. 63 (2011) 789–808, https://doi.org/10.1016/j.addr.2011.03.008.
[32] K.E. Scarberry, E.B. Dickerson, J.F. McDonald, Z.J. Zhang, Magnetic nanoparticle-peptide conjugates for *in vitro* and *in vivo* targeting and extraction of cancer cells, J. Am. Chem. Soc. 130 (2008) 10258–10262, https://doi.org/10.1021/ja801969b.
[33] K.E. Scarberry, R. Mezencev, J.F. McDonald, Targeted removal of migratory tumor cells by functionalized magnetic nanoparticles impedes metastasis and tumor progression, Nanomedicine 6 (2011) 69–78, https://doi.org/10.2217/nnm.10.103.
[34] P. Kaur, M.L. Aliru, A.S. Chadha, A. Asea, S. Krishnan, Hyperthermia using nanoparticles – promises and pitfalls, Int. J. Hyperth. 32 (2016) 76–88, https://doi.org/10.3109/02656736.2015.1120889.
[35] P. Makvandi, C. Wang, E.N. Zare, A. Borzacchiello, L. Niu, F.R. Tay, Metal-based nanomaterials in biomedical applications: antimicrobial activity and cytotoxicity aspects, Adv. Funct. Mater. 30 (2020), 1910021, https://doi.org/10.1002/adfm.201910021.
[36] P. Tran, S.E. Lee, D.H. Kim, Y.C. Pyo, J.S. Park, Recent advances of nanotechnology for the delivery of anticancer drugs for breast cancer treatment, J. Pharm. Investig. 50 (2020) 261–270, https://doi.org/10.1007/s40005-019-00459-7.
[37] S. Talegaonkar, A. Bhattacharyya, Potential of lipid nanoparticles (SLNs and NLCs) in enhancing oral bioavailability of drugs with poor intestinal permeability, AAPS PharmSciTech 20 (2019) 121, https://doi.org/10.1208/s12249-019-1337-8.
[38] D.R. Bielenberg, B.R. Zetter, The contribution of angiogenesis to the process of metastasis, Cancer J. 21 (2015) 267–273, https://doi.org/10.1097/PPO.0000000000000138.
[39] B. Haley, E. Frenkel, Nanoparticles for drug delivery in cancer treatment, Urol. Oncol. Semin. Orig. Investig. 26 (2008) 57–64, https://doi.org/10.1016/j.urolonc.2007.03.015.
[40] D. Huang, H. Lan, F. Liu, S. Wang, X. Chen, K. Jin, X. Mou, Anti-angiogenesis or pro-angiogenesis for cancer treatment: focus on drug distribution, Int. J. Clin. Exp. Med. 8 (2015) 8369–8376. http://www.ncbi.nlm.nih.gov/pubmed/26309490.
[41] S.K. Golombek, J. May, B. Theek, L. Appold, N. Drude, F. Kiessling, T. Lammers, Tumor targeting via EPR: Strategies to enhance patient responses, Adv. Drug Deliv. Rev. 130 (2018) 17–38, https://doi.org/10.1016/j.addr.2018.07.007.
[42] J. Park, Y. Choi, H. Chang, W. Um, J.H. Ryu, I.C. Kwon, Alliance with EPR effect: combined strategies to improve the EPR effect in the tumor microenvironment, Theranostics 9 (2019) 8073–8090, https://doi.org/10.7150/thno.37198.
[43] A.K. Pearce, R.K. O'Reilly, Insights into active targeting of nanoparticles in drug delivery: advances in clinical studies and design considerations for cancer nanomedicine, Bioconjug. Chem. 30 (2019) 2300–2311, https://doi.org/10.1021/acs.bioconjchem.9b00456.
[44] D. Peer, Harnessing RNAi nanomedicine for precision therapy, Mol. Cell. Ther. 2 (2014) 5, https://doi.org/10.1186/2052-8426-2-5.
[45] G. Bozzuto, A. Molinari, Liposomes as nanomedical devices, Int. J. Nanomed. 10 (2015) 975, https://doi.org/10.2147/IJN.S68861.
[46] H. Kobayashi, B. Turkbey, R. Watanabe, P.L. Choyke, Cancer drug delivery: considerations in the rational design of nanosized bioconjugates, Bioconjug. Chem. 25 (2014) 2093–2100, https://doi.org/10.1021/bc500481x.
[47] T. Asai, Nanoparticle-mediated delivery of anticancer agents to tumor angiogenic vessels, Biol. Pharm. Bull. 35 (2012) 1855–1861, https://doi.org/10.1248/bpb.b212013.
[48] A. Schroeder, D.A. Heller, M.M. Winslow, J.E. Dahlman, G.W. Pratt, R. Langer, T. Jacks, D.G. Anderson, Treating metastatic cancer with nanotechnology, Nat. Rev. Cancer. 12 (2012) 39–50, https://doi.org/10.1038/nrc3180.
[49] M. Ghafari, F. Haghiralsadat, S. Khanamani Falahati-pour, J. Zavar Reza, Development of a novel liposomal nanoparticle formulation of cisplatin to breast cancer therapy, J. Cell. Biochem. 121 (2020) 3584–3592, https://doi.org/10.1002/jcb.29651.
[50] Y. Hui, X. Yi, F. Hou, D. Wibowo, F. Zhang, D. Zhao, H. Gao, C.X. Zhao, Role of nanoparticle mechanical properties in cancer drug delivery, ACS Nano 13 (2019) 7410–7424, https://doi.org/10.1021/acsnano.9b03924.
[51] R.P. Das, V.V Gandhi, B.G. Singh, A. Kunwar, Passive and active drug targeting: role of nanocarriers in rational design of anticancer formulations, Curr. Pharm. Des. 25 (2019) 3034–3056, https://doi.org/10.2174/1381612825666190830155319.
[52] C. Senthil Kumar, R. Thangam, S.A. Mary, P.R. Kannan, G. Arun, B. Madhan, Targeted delivery and apoptosis induction of trans-resveratrol-ferulic acid loaded chitosan coated folic acid conjugate solid lipid nanoparticles in colon cancer cells, Carbohydr. Polym. 231 (2020), 115682, https://doi.org/10.1016/j.carbpol.2019.115682.
[53] Y. Li, J. Lin, X. Yang, Y. Li, S. Wu, Y. Huang, S. Ye, L. Xie, L. Dai, Z. Hou, Self-assembled nanoparticles based on amphiphilic anticancer drug–phospholipid complex for targeted drug delivery and intracellular dual-controlled release, ACS Appl. Mater. Interfaces 7 (2015) 17573–17581, https://doi.org/10.1021/acsami.5b05038.
[54] R. Shukla, M. Handa, S.B. Lokesh, M. Ruwali, K. Kohli, P. Kesharwani, Conclusion and future prospective of polymeric nanoparticles for cancer therapy. Polymeric Nanoparticles as a Promising Tool for Anti-cancer Therapeutics, Elsevier, 2019, pp. 389–408, https://doi.org/10.1016/B978-0-12-816963-6.00018-2.
[55] J.P. Abriata, R.C. Turatti, M.T. Luiz, G.L. Raspantini, L.B. Tofani, R.L.F. do Amaral, K. Swiech, P.D. Marcato, J.M. Marchetti, Development, characterization and biological *in vitro* assays of paclitaxel-loaded PCL polymeric nanoparticles, Mater. Sci. Eng. C 96 (2019) 347–355, https://doi.org/10.1016/j.msec.2018.11.035.
[56] Y. Alyassin, E.G. Sayed, P. Mehta, K. Ruparelia, M.S. Arshad, M. Rasekh, J. Shepherd, I. Kucuk, P.B. Wilson, N. Singh, M.W. Chang, D.G. Fatouros, Z. Ahmad, Application of mesoporous silica nanoparticles as drug delivery carriers for chemotherapeutic agents, Drug Discov. Today 25 (2020) 1513–1520, https://doi.org/10.1016/j.drudis.2020.06.006.
[57] N. Lu, Y. Tian, W. Tian, P. Huang, Y. Liu, Y. Tang, C. Wang, S. Wang, Y. Su, Y. Zhang, J. Pan, Z. Teng, G. Lu, Smart cancer cell targeting imaging and drug delivery system by systematically engineering periodic mesoporous organosilica nanoparticles, ACS Appl. Mater. Interfaces 8 (2016) 2985–2993, https://doi.org/10.1021/acsami.5b09585.
[58] Y. Hadadian, A.P. Ramos, T.Z. Pavan, Role of zinc substitution in magnetic hyperthermia properties of magnetite nanoparticles: interplay between intrinsic properties and dipolar interactions, Sci. Rep. 9 (2019) 18048, https://doi.org/10.1038/s41598-019-54250-7.
[59] Z. Karimi, S. Abbasi, H. Shokrollahi, G. Yousefi, M. Fahham, L. Karimi, O. Firuzi, Pegylated and amphiphilic chitosan coated manganese ferrite nanoparticles for pH-sensitive delivery of methotrexate: synthesis and characterization, Mater. Sci. Eng. C 71 (2017) 504–511, https://doi.org/10.1016/j.msec.2016.10.008.
[60] C. Iacovita, A. Florea, L. Scorus, E. Pall, R. Dudric, A.I. Moldovan, R. Stiufiuc, R. Tetean, C.M. Lucaciu, Hyperthermia, cytotoxicity, and cellular uptake properties of manganese and zinc ferrite magnetic nanoparticles synthesized by a polyol-mediated process, Nanomaterials 9 (2019) 1489, https://doi.org/10.3390/nano9101489.
[61] J. Wang, Y. Zhang, L. Liu, Z. Cui, X. Liu, L. Wang, Y. Li, Q. Li, Combined chemo/photothermal therapy based on mesoporous silica-Au core-shell nanoparticles for hepatocellular carcinoma treatment, Drug Dev. Ind. Pharm. 45 (2019) 1487–1495, https://doi.org/10.1080/03639045.2019.1629688.
[62] J.H. Lee, J. Jang, J. Choi, S.H. Moon, S. Noh, J. Kim, J.G. Kim, I.S. Kim, K.I. Park, J. Cheon, Exchange-coupled magnetic nanoparticles for efficient heat induction, Nat. Nanotechnol. 6 (2011) 418–422, https://doi.org/10.1038/nnano.2011.95.

[63] J. Jose, R. Kumar, S. Harilal, G.E. Mathew, D.G.T. Parambi, A. Prabhu, M. S. Uddin, L. Aleya, H. Kim, B. Mathew, Magnetic nanoparticles for hyperthermia in cancer treatment: an emerging tool, Environ. Sci. Pollut. Res. 27 (2020) 19214–19225, https://doi.org/10.1007/s11356-019-07231-2.

[64] P. Das, M. Colombo, D. Prosperi, Recent advances in magnetic fluid hyperthermia for cancer therapy, Colloids Surfaces B Biointerfaces 174 (2019) 42–55, https://doi.org/10.1016/j.colsurfb.2018.10.051.

[65] J. Huang, Y. Li, A. Orza, Q. Lu, P. Guo, L. Wang, L. Yang, H. Mao, Magnetic nanoparticle facilitated drug delivery for cancer therapy with targeted and image-guided approaches, Adv. Funct. Mater. 26 (2016) 3818–3836, https://doi.org/10.1002/adfm.201504185.

[66] X. Zhang, Y. Zhang, Experimental study on enhanced heat transfer and flow performance of magnetic nanofluids under alternating magnetic field, Int. J. Therm. Sci. 164 (2021), 106897, https://doi.org/10.1016/j.ijthermalsci.2021.106897.

[67] L. Cheng, C. Wang, L. Feng, K. Yang, Z. Liu, Functional nanomaterials for phototherapies of cancer, Chem. Rev. 114 (2014) 10869–10939, https://doi.org/10.1021/cr400532z.

[68] H. Wu, L. Liu, L. Song, M. Ma, N. Gu, Y. Zhang, Enhanced tumor synergistic therapy by injectable magnetic hydrogel mediated generation of hyperthermia and highly toxic reactive oxygen species, ACS Nano 13 (2019) 14013–14023, https://doi.org/10.1021/acsnano.9b06134.

[69] M-H. Chan, M-R. Hsieh, R-S. Liu, D-H. Wei, M. Hsiao, Magnetically Guided Theranostics: Optimizing Magnetic Resonance Imaging with Sandwich-Like Kaolinite-Based Iron/Platinum Nanoparticles for Magnetic Fluid Hyperthermia and Chemotherapy, Chem. Mater. 32 (2) (2020) 697–708, https://doi.org/10.1021/acs.chemmater.9b03552.

[70] X. Liu, B. Yan, Y. Li, X. Ma, W. Jiao, K. Shi, T. Zhang, S. Chen, Y. He, X. Liang, H. Fan, Graphene oxide-grafted magnetic nanorings mediated magnetothermodynamic therapy favoring reactive oxygen species-related immune response for enhanced antitumor efficacy, ACS Nano 14 (2020) 1936–1950, https://doi.org/10.1021/acsnano.9b08320.

[71] Y. Wang, L. Zou, Z. Qiang, J. Jiang, Z. Zhu, J. Ren, Enhancing targeted cancer treatment by combining hyperthermia and radiotherapy using Mn–Zn ferrite magnetic nanoparticles, ACS Biomater. Sci. Eng. 6 (2020) 3550–3562, https://doi.org/10.1021/acsbiomaterials.0c00287.

[72] S.M. Carvalho, A.G. Leonel, A.A.P. Mansur, I.C. Carvalho, K. Krambrock, H. S. Mansur, Bifunctional magnetopolymersomes of iron oxide nanoparticles and carboxymethylcellulose conjugated with doxorubicin for hyperthermo-chemotherapy of brain cancer cells, Biomater. Sci. 7 (2019) 2102–2122, https://doi.org/10.1039/C8BM01528G.

[73] E. Augustin, B. Czubek, A.M. Nowicka, A. Kowalczyk, Z. Stojek, Z. Mazerska, Improved cytotoxicity and preserved level of cell death induced in colon cancer cells by doxorubicin after its conjugation with iron-oxide magnetic nanoparticles, Toxicol. *In Vitro* 33 (2016) 45–53, https://doi.org/10.1016/j.tiv.2016.02.009.

[74] M. Rahimi, K.D. Safa, R. Salehi, Co-delivery of doxorubicin and methotrexate by dendritic chitosan-g-mPEG as a magnetic nanocarrier for multi-drug delivery in combination chemotherapy, Polym. Chem. 8 (2017) 7333–7350, https://doi.org/10.1039/C7PY01701D.

[75] X. Li, X. Wang, L. Sha, D. Wang, W. Shi, Q. Zhao, S. Wang, Thermosensitive lipid bilayer-coated mesoporous carbon nanoparticles for synergistic thermochemotherapy of tumor, ACS Appl. Mater. Interfaces 10 (2018) 19386–19397, https://doi.org/10.1021/acsami.8b03008.

[76] N. Lu, P. Huang, W. Fan, Z. Wang, Y. Liu, S. Wang, G. Zhang, J. Hu, W. Liu, G. Niu, R.D. Leapman, G. Lu, X. Chen, Tri-stimuli-responsive biodegradable theranostics for mild hyperthermia enhanced chemotherapy, Biomaterials 126 (2017) 39–48, https://doi.org/10.1016/j.biomaterials.2017.02.025.

[77] M.A. Miller, H. Mikula, G. Luthria, R. Li, S. Kronister, M. Prytyskach, R.H. Kohler, T. Mitchison, R. Weissleder, Modular nanoparticulate prodrug design enables efficient treatment of solid tumors using bioorthogonal activation, ACS Nano 12 (2018) 12814–12826, https://doi.org/10.1021/acsnano.8b07954.

[78] X. Xie, L. Zhang, W. Zhang, R. Tayebee, A. Hoseininasr, H.H. Vatanpour, Z. Behjati, S. Li, M. Nasrabadi, L. Liu, Fabrication of temperature and pH sensitive decorated magnetic nanoparticles as effective biosensors for targeted delivery of acyclovir anti-cancer drug, J. Mol. Liq. 309 (2020), 113024, https://doi.org/10.1016/j.molliq.2020.113024.

[79] K. El-Boubbou, Magnetic iron oxide nanoparticles as drug carriers: clinical relevance, Nanomedicine 13 (2018) 953–971, https://doi.org/10.2217/nnm-2017-0336.

[80] Y.I. Jeong, S.G. Jin, I.Y. Kim, J. Pei, M. Wen, T.Y. Jung, K.S. Moon, S. Jung, Doxorubicin-incorporated nanoparticles composed of poly(ethylene glycol)-grafted carboxymethyl chitosan and antitumor activity against glioma cells *in vitro*, Colloids Surfaces B Biointerfaces 79 (2010) 149–155, https://doi.org/10.1016/j.colsurfb.2010.03.037.

[81] C.H. Huang, T.J. Chuang, C.J. Ke, C.H. Yao, Doxorubicin–Gelatin/Fe_3O_4–Alginate dual-layer magnetic nanoparticles as targeted anticancer drug delivery vehicles, Polymers 12 (2020) 1747, https://doi.org/10.3390/polym12081747 (Basel).

[82] W. Hulangamuwa, B. Acharya, V. Chikan, R.J. Rafferty, Triggering passive molecular transport into cells with a combination of inhomogeneous magnetic fields and magnetic nanoparticles, ACS Appl. Nano Mater. 3 (2020) 2414–2420, https://doi.org/10.1021/acsanm.9b02537.

[83] L. Jie, D. Lang, X. Kang, Z. Yang, Y. Du, X. Ying, Superparamagnetic iron oxide nanoparticles/doxorubicin-loaded starch-octanoic micelles for targeted tumor therapy, J. Nanosci. Nanotechnol. 19 (2019) 5456–5462, https://doi.org/10.1166/jnn.2019.16548.

[84] J. Mosafer, K. Abnous, M. Tafaghodi, A. Mokhtarzadeh, M. Ramezani, *In vitro* and *in vivo* evaluation of anti-nucleolin-targeted magnetic PLGA nanoparticles loaded with doxorubicin as a theranostic agent for enhanced targeted cancer imaging and therapy, Eur. J. Pharm. Biopharm. 113 (2017) 60–74, https://doi.org/10.1016/j.ejpb.2016.12.009.

[85] L. Lerra, A. Farfalla, B. Sanz, G. Cirillo, O. Vittorio, F. Voli, M.Le Grand, M. Curcio, F. Nicoletta, A. Dubrovska, S. Hampel, F. Iemma, G. Goya, Graphene oxide functional nanohybrids with magnetic nanoparticles for improved vectorization of doxorubicin to neuroblastoma cells, Pharmaceutics 11 (2018) 3, https://doi.org/10.3390/pharmaceutics11010003.

[86] C. Shen, X. Wang, Z. Zheng, C. Gao, X. Chen, S. Zhao, Z. Dai, Doxorubicin and indocyanine green loaded superparamagnetic iron oxide nanoparticles with PEGylated phospholipid coating for magnetic resonance with fluorescence imaging and chemotherapy of glioma, Int. J. Nanomed. Vol. 14 (2018) 101–117, https://doi.org/10.2147/IJN.S173954.

[87] J. Chen, M. Shi, P. Liu, A. Ko, W. Zhong, W. Liao, M.M.Q. Xing, Reducible polyamidoamine-magnetic iron oxide self-assembled nanoparticles for doxorubicin delivery, Biomaterials 35 (2014) 1240–1248, https://doi.org/10.1016/j.biomaterials.2013.10.057.

[88] N. Avedian, F. Zaaeri, M.P. Daryasari, H. Akbari Javar, M. Khoobi, pH-sensitive biocompatible mesoporous magnetic nanoparticles labeled with folic acid as an efficient carrier for controlled anticancer drug delivery, J. Drug Deliv. Sci. Technol. 44 (2018) 323–332, https://doi.org/10.1016/j.jddst.2018.01.006.

[89] M. Fathi, J. Barar, H. Erfan-Niya, Y. Omidi, Methotrexate-conjugated chitosan-grafted pH- and thermo-responsive magnetic nanoparticles for targeted therapy of ovarian cancer, Int. J. Biol. Macromol. 154 (2020) 1175–1184, https://doi.org/10.1016/j.ijbiomac.2019.10.272.

[90] H. Han, Y. Hou, X. Chen, P. Zhang, M. Kang, Q. Jin, J. Ji, M. Gao, Metformin-induced stromal depletion to enhance the penetration of gemcitabine-loaded magnetic nanoparticles for pancreatic cancer targeted therapy, J. Am. Chem. Soc. 142 (2020) 4944–4954, https://doi.org/10.1021/jacs.0c00650.

[91] J. Lin, Y. Li, Y. Li, H. Wu, F. Yu, S. Zhou, L. Xie, F. Luo, C. Lin, Z. Hou, Drug/dye-loaded, multifunctional PEG–chitosan–iron oxide nanocomposites for methotraxate synergistically self-targeted cancer therapy and dual model imaging, ACS Appl. Mater. Interfaces 7 (2015) 11908–11920, https://doi.org/10.1021/acsami.5b01685.

[92] M.A. Vakilinezhad, S. Alipour, H. Montaseri, Fabrication and *in vitro* evaluation of magnetic PLGA nanoparticles as a potential Methotrexate delivery system for breast cancer, J. Drug Deliv. Sci. Technol. 44 (2018) 467–474, https://doi.org/10.1016/j.jddst.2018.01.002.

[93] H.R. Naghibi Beidokhti, R. Ghaffarzadegan, S. Mirzakhanlouei, L. Ghazizadeh, F. A. Dorkoosh, Preparation, characterization, and optimization of folic acid-chitosan-methotrexate core-shell nanoparticles by box-behnken design for tumor-targeted drug delivery, AAPS PharmSciTech 18 (2017) 115–129, https://doi.org/10.1208/s12249-015-0445-3.

[94] R.P. Dhavale, R.P. Dhavale, S.C. Sahoo, P. Kollu, S.U. Jadhav, P.S. Patil, T. D. Dongale, A.D. Chougale, P.B. Patil, Chitosan coated magnetic nanoparticles as carriers of anticancer drug telmisartan: pH-responsive controlled drug release and cytotoxicity studies, J. Phys. Chem. Solids 148 (2021), 109749, https://doi.org/10.1016/j.jpcs.2020.109749.

[95] K.S. Joshy, R. Augustine, A. Mayeen, S.M. Alex, A. Hasan, S. Thomas, H. Chi, $NiFe_2O_4$ /poly(ethylene glycol)/lipid–polymer hybrid nanoparticles for anti-cancer drug delivery, New J. Chem. 44 (2020) 18162–18172, https://doi.org/10.1039/D0NJ01163K.

[96] F. Wu, B. Sun, X. Chu, Q. Zhang, Z. She, S. Song, N. Zhou, J. Zhang, X. Yi, D. Wu, J. Wang, Hyaluronic acid-modified porous carbon-coated Fe_3O_4 nanoparticles for magnetic resonance imaging-guided photothermal/chemotherapy of tumors, Langmuir 35 (2019) 13135–13144, https://doi.org/10.1021/acs.langmuir.9b02300.

[97] B.T. Mai, P.B. Balakrishnan, M.J. Barthel, F. Piccardi, D. Niculaes, F. Marinaro, S. Fernandes, A. Curcio, H. Kakwere, G. Autret, R. Cingolani, F. Gazeau, T. Pellegrino, Thermoresponsive iron oxide nanocubes for an effective clinical translation of magnetic hyperthermia and heat-mediated chemotherapy, ACS Appl. Mater. Interfaces 11 (2019) 5727–5739, https://doi.org/10.1021/acsami.8b16226.

[98] T.S. Anirudhan, J. Christa, Temperature and pH sensitive multi-functional magnetic nanocomposite for the controlled delivery of 5-fluorouracil, an anticancer drug, J. Drug Deliv. Sci. Technol. 55 (2020), 101476, https://doi.org/10.1016/j.jddst.2019.101476.

[99] P. Appa Rao, K. Srinivasa Rao, T.R.K. Pydi Raju, G. Kapusetti, M. Choppadandi, M. Chaitanya Varma, K.H. Rao, A systematic study of cobalt-zinc ferrite nanoparticles for self-regulated magnetic hyperthermia, J. Alloys Compd. 794 (2019) 60–67, https://doi.org/10.1016/j.jallcom.2019.04.242.

[100] M. Horny, J. Gamby, V. Dupuis, J. Siaugue, Magnetic Hyperthermia on γ-Fe_2O_3@SiO_2 Core-Shell Nanoparticles for mi-RNA 122 Detection, Nanomaterials 11 (2021) 149, https://doi.org/10.3390/nano11010149.

[101] S. Mondal, P. Manivasagan, S. Bharathiraja, M. Santha Moorthy, V. Nguyen, H. Kim, S. Nam, K. Lee, J. Oh, Hydroxyapatite coated iron oxide nanoparticles: a promising nanomaterial for magnetic hyperthermia cancer treatment, Nanomaterials 7 (2017) 426, https://doi.org/10.3390/nano7120426.

[102] A. Makridis, K. Topouridou, M. Tziomaki, D. Sakellari, K. Simeonidis, M. Angelakeris, M..P. Yavropoulou, J.G. Yovos, O. Kalogirou, *In vitro* application of Mn-ferrite nanoparticles as novel magnetic hyperthermia agents, J. Mater. Chem. B 2 (2014) 8390–8398, https://doi.org/10.1039/C4TB01017E.

[103] J. Xie, Y. Zhang, C. Yan, L. Song, S. Wen, F. Zang, G. Chen, Q. Ding, C. Yan, N. Gu, High-performance PEGylated Mn–Zn ferrite nanocrystals as a passive-targeted

agent for magnetically induced cancer theranostics, Biomaterials 35 (2014) 9126–9136, https://doi.org/10.1016/j.biomaterials.2014.07.019.
[104] J. Jang, J. Lee, J. Seon, E. Ju, M. Kim, Y. Il Kim, M.G. Kim, Y. Takemura, A. S. Arbab, K.W. Kang, K.H. Park, S.H. Paek, S. Bae, Giant magnetic heat induction of magnesium-doped γ-Fe_2O_3 Superparamagnetic nanoparticles for completely killing tumors, Adv. Mater. 30 (2018), 1704362, https://doi.org/10.1002/adma.201704362.
[105] Y. Ling, X. Tang, F. Wang, X. Zhou, R. Wang, L. Deng, T. Shang, B. Liang, P. Li, H. Ran, Z. Wang, B. Hu, C. Li, G. Zuo, Y. Zheng, Highly efficient magnetic hyperthermia ablation of tumors using injectable polymethylmethacrylate–Fe_3O_4, RSC Adv. 7 (2017) 2913–2918, https://doi.org/10.1039/C6RA20860F.
[106] F. Wang, Y. Yang, Y. Ling, J. Liu, X. Cai, X. Zhou, X. Tang, B. Liang, Y. Chen, H. Chen, D. Chen, C. Li, Z. Wang, B. Hu, Y. Zheng, Injectable and thermally contractible hydroxypropyl methyl cellulose/Fe_3O_4 for magnetic hyperthermia ablation of tumors, Biomaterials 128 (2017) 84–93, https://doi.org/10.1016/j.biomaterials.2017.03.004.
[107] R.J. Wydra, P.G. Rychahou, B.M. Evers, K.W. Anderson, T.D. Dziubla, J.Z. Hilt, The role of ROS generation from magnetic nanoparticles in an alternating magnetic field on cytotoxicity, Acta Biomater. 25 (2015) 284–290, https://doi.org/10.1016/j.actbio.2015.06.037.
[108] O.L. Lanier, O.I. Korotych, A.G. Monsalve, D. Wable, S. Savliwala, N.W. F. Grooms, C. Nacea, O.R. Tuitt, J. Dobson, Evaluation of magnetic nanoparticles for magnetic fluid hyperthermia, Int. J. Hyperth. 36 (2019) 686–700, https://doi.org/10.1080/02656736.2019.1628313.
[109] E. Guisasola, L. Asín, L. Beola, J.M. de la Fuente, A. Baeza, M. Vallet-Regí, Beyond traditional hyperthermia: *in vivo* cancer treatment with magnetic-responsive mesoporous silica nanocarriers, ACS Appl. Mater. Interfaces 10 (2018) 12518–12525, https://doi.org/10.1021/acsami.8b02398.
[110] S. Kobayashi, A. Ohki, M. Tanoue, Y. Inaoka, K. Murase, Comparative study of extracellular and intracellular magnetic hyperthermia treatments using magnetic particle imaging, Open J. Appl. Sci. 07 (2017) 647–660, https://doi.org/10.4236/ojapps.2017.712047.
[111] K.S. Kim, J. Kim, J.Y. Lee, S. Matsuda, S. Hideshima, Y. Mori, T. Osaka, K. Na, Stimuli-responsive magnetic nanoparticles for tumor-targeted bimodal imaging and photodynamic/hyperthermia combination therapy, Nanoscale 8 (2016) 11625–11634, https://doi.org/10.1039/C6NR02273A.
[112] L. Sun, D.Y. Joh, A. Al-Zaki, M. Stangl, S. Murty, J.J. Davis, B.C. Baumann, M. Alonso-Basanta, G.D. Kao, A. Tsourkas, J.F. Dorsey, Theranostic application of mixed gold and superparamagnetic iron oxide nanoparticle micelles in glioblastoma multiforme, J. Biomed. Nanotechnol. 12 (2016) 347–356, https://doi.org/10.1166/jbn.2016.2173.
[113] A. Aires, S.M. Ocampo, B.M. Simões, M.Josefa Rodríguez, J.F. Cadenas, P. Couleaud, K. Spence, A. Latorre, R. Miranda, Á. Somoza, R.B. Clarke, J. L. Carrascosa, A.L. Cortajarena, Multifunctionalized iron oxide nanoparticles for selective drug delivery to CD44-positive cancer cells, Nanotechnology 27 (2016), 065103, https://doi.org/10.1088/0957-4484/27/6/065103.
[114] L. Rao, B. Cai, L.L. Bu, Q.Q. Liao, S.S. Guo, X.Z. Zhao, W.F. Dong, W. Liu, Microfluidic electroporation-facilitated synthesis of erythrocyte membrane-coated magnetic nanoparticles for enhanced imaging-guided cancer therapy, ACS Nano 11 (2017) 3496–3505, https://doi.org/10.1021/acsnano.7b00133.
[115] H. Kalita, S. Rajput, B.N.P. Kumar, M. Mandal, A. Pathak, Fe_3O_4 @zirconium phosphate core–shell nanoparticles for pH-sensitive and magnetically guided drug delivery applications, RSC Adv. 6 (2016) 21285–21292, https://doi.org/10.1039/C5RA27215G.
[116] C. Caizer, Optimization study on specific loss power in superparamagnetic hyperthermia with magnetite nanoparticles for high efficiency in alternative cancer therapy, Nanomaterials 11 (2020) 40, https://doi.org/10.3390/nano11010040.
[117] M. Grabowska, B.F. Grześkowiak, K. Szutkowski, D. Wawrzyniak, P. Głodowicz, J. Barciszewski, S. Jurga, K. Rolle, R. Mrówczyński, Nano-mediated delivery of double-stranded RNA for gene therapy of glioblastoma multiforme, PLoS One 14 (2019), e0213852, https://doi.org/10.1371/journal.pone.0213852.
[118] M. Busquets, A. Espargaró, R. Sabaté, J. Estelrich, Magnetic nanoparticles cross the blood-brain barrier: when physics rises to a challenge, Nanomaterials 5 (2015) 2231–2248, https://doi.org/10.3390/nano5042231.
[119] S. Sayadnia, E. Arkan, R. Jahanban-Esfahlan, S. Sayadnia, M. Jaymand, Tragacanth gum-based pH-responsive magnetic hydrogels for “smart” chemo/hyperthermia therapy of solid tumors, Polym. Adv. Technol. 32 (2021) 262–271, https://doi.org/10.1002/pat.5082.
[120] P. He, Z. Wang, L. Zhang, W. Yang, Development of a label-free electrochemical immunosensor based on carbon nanotube for rapid determination of clenbuterol, Food Chem. 112 (2009) 707–714, https://doi.org/10.1016/j.foodchem.2008.05.116.
[121] S.E. Kim, M. Van Tieu, S.Y. Hwang, M.H. Lee, Magnetic particles: their applications from sample preparations to biosensing platforms, Micromachines 11 (2020) 302, https://doi.org/10.3390/mi11030302.
[122] Y. Jin, X. Yao, Q. Liu, J. Li, Hairpin DNA probe based electrochemical biosensor using methylene blue as hybridization indicator, Biosens. Bioelectron. 22 (2007) 1126–1130, https://doi.org/10.1016/j.bios.2006.04.011.
[123] World Health Organization, Safety International Programme on Chemical. Biomarkers in risk assessment : validity and validation, World Health Organization, 2001. https://apps.who.int/iris/handle/10665/42363.
[124] Z. Taleat, A. Ravalli, M. Mazloum-Ardakani, G. Marrazza, CA 125 Immunosensor based on poly-anthranilic acid modified screen-printed electrodes, Electroanalysis 25 (2013) 269–277, https://doi.org/10.1002/elan.201200425.
[125] J. López, L.F. González-Bahamón, J. Prado, J.C. Caicedo, G. Zambrano, M. E. Gómez, J. Esteve, P. Prieto, Study of magnetic and structural properties of ferrofluids based on cobalt–zinc ferrite nanoparticles, J. Magn. Magn. Mater. 324 (2012) 394–402, https://doi.org/10.1016/j.jmmm.2011.07.040.
[126] J. Liu, Z. Sun, Y. Deng, Y. Zou, C. Li, X. Guo, L. Xiong, Y. Gao, F. Li, D. Zhao, Highly water-dispersible biocompatible magnetite particles with low cytotoxicity stabilized by citrate groups, Angew. Chemie Int. Ed. 48 (2009) 5875–5879, https://doi.org/10.1002/anie.200901566.
[127] M. Pastucha, Z. Farka, K. Lacina, Z. Mikušová, P. Skládal, Magnetic nanoparticles for smart electrochemical immunoassays: a review on recent developments, Microchim. Acta 186 (2019) 312, https://doi.org/10.1007/s00604-019-3410-0.
[128] Z. Farka, T. Jurík, D. Kovář, L. Trnková, P. Skládal, Nanoparticle-based immunochemical biosensors and assays: recent advances and challenges, Chem. Rev. 117 (2017) 9973–10042, https://doi.org/10.1021/acs.chemrev.7b00037.
[129] T.A.P. Rocha-Santos, Sensors and biosensors based on magnetic nanoparticles, TrAC Trends Anal. Chem. 62 (2014) 28–36, https://doi.org/10.1016/j.trac.2014.06.016.
[130] A.E. Urusov, A.V Petrakova, A.V Zherdev, B.B. Dzantiev, Application of magnetic nanoparticles in immunoassay, Nanotechnol. Russ 12 (2017) 471–479, https://doi.org/10.1134/S1995078017050135.
[131] Tertis Hosu, Cristea, Implication of magnetic nanoparticles in cancer detection, screening and treatment, Magnetochemistry 5 (2019) 55, https://doi.org/10.3390/magnetochemistry5040055.
[132] M. Fathi, S. Majidi, P.S. Zangabad, J. Barar, H. Erfan-Niya, Y. Omidi, Chitosan-based multifunctional nanomedicines and theranostics for targeted therapy of cancer, Med. Res. Rev. 38 (2018) 2110–2136, https://doi.org/10.1002/med.21506.
[133] K. Donadel, M.D.V. Felisberto, V.T. Fávere, M. Rigoni, N.J. Batistela, M.C. M. Laranjeira, Synthesis and characterization of the iron oxide magnetic particles coated with chitosan biopolymer, Mater. Sci. Eng. C 28 (2008) 509–514, https://doi.org/10.1016/j.msec.2007.06.004.
[134] A.S. Afonso, C.V. Uliana, D.H. Martucci, R.C. Faria, Simple and rapid fabrication of disposable carbon-based electrochemical cells using an electronic craft cutter for sensor and biosensor applications, Talanta 146 (2016) 381–387, https://doi.org/10.1016/j.talanta.2015.09.002.
[135] C.V. Uliana, C.R. Peverari, A.S. Afonso, M.R. Cominetti, R.C. Faria, Fully disposable microfluidic electrochemical device for detection of estrogen receptor alpha breast cancer biomarker, Biosens. Bioelectron. 99 (2018) 156–162, https://doi.org/10.1016/j.bios.2017.07.043.
[136] J. Biscay, M.B. González García, A.C. García, Determination of total PSA using magnetic beads and a re-usable screen printed carbon electrode array, Electroanalysis 27 (2015) 2773–2777, https://doi.org/10.1002/elan.201500351.
[137] Z. Rashid, M. Soleimani, R. Ghahremanzadeh, M. Vossoughi, E. Esmaeili, Effective surface modification of $MnFe_2O_4$ @SiO_2 @PMIDA magnetic nanoparticles for rapid and high-density antibody immobilization, Appl. Surf. Sci. 426 (2017) 1023–1029, https://doi.org/10.1016/j.apsusc.2017.07.246.
[138] V. Mani, B.V. Chikkaveeraiah, V. Patel, J.S. Gutkind, J.F. Rusling, Ultrasensitive immunosensor for cancer biomarker proteins using gold nanoparticle film electrodes and multienzyme-particle amplification, ACS Nano 3 (2009) 585–594, https://doi.org/10.1021/nn800863w.
[139] B.A. Otieno, C.E. Krause, A. Latus, B.V. Chikkaveeraiah, R.C. Faria, J.F. Rusling, On-line protein capture on magnetic beads for ultrasensitive microfluidic immunoassays of cancer biomarkers, Biosens. Bioelectron. 53 (2014) 268–274, https://doi.org/10.1016/j.bios.2013.09.054.
[140] L. Morán, F.J. Cubero, Extracellular vesicles in liver disease and beyond, World J. Gastroenterol. 24 (2018) 4519–4526, https://doi.org/10.3748/wjg.v24.i40.4519.
[141] P. Li, X. Yu, W. Han, Y. Kong, W. Bao, J. Zhang, W. Zhang, Y. Gu, Ultrasensitive and reversible nanoplatform of urinary exosomes for prostate cancer diagnosis, ACS Sens. 4 (2019) 1433–1441, https://doi.org/10.1021/acssensors.9b00621.
[142] C.Z.J. Lim, L. Zhang, Y. Zhang, N.R. Sundah, H. Shao, New sensors for extracellular vesicles: insights on constituent and associated biomarkers, ACS Sens. 5 (2020) 4–12, https://doi.org/10.1021/acssensors.9b02165.
[143] S.L. Moura, C.G. Martín, M. Martí, M.I. Pividori, Electrochemical immunosensing of nanovesicles as biomarkers for breast cancer, Biosens. Bioelectron. 150 (2020), 111882, https://doi.org/10.1016/j.bios.2019.111882.
[144] S.L. Moura, C.G. Martín, M. Martí, M.I. Pividori, Multiplex detection and characterization of breast cancer exosomes by magneto-actuated immunoassay, Talanta 211 (2020), 120657, https://doi.org/10.1016/j.talanta.2019.120657.
[145] S. Lima Moura, M. Martì, M.I. Pividori, Matrix effect in the isolation of breast cancer-derived nanovesicles by immunomagnetic separation and electrochemical Immunosensing – a comparative study, Sensors 20 (2020) 965, https://doi.org/10.3390/s20040965.
[146] Y. Zhao, X. Cai, C. Zhu, H. Yang, D. Du, A novel fluorescent and electrochemical dual-responsive immunosensor for sensitive and reliable detection of biomarkers based on cation-exchange reaction, Anal. Chim. Acta. 1096 (2020) 61–68, https://doi.org/10.1016/j.aca.2019.10.054.
[147] G. Volpe, R. Draisci, G. Palleschi, D. Compagnone, 3,3′,5,5′-Tetramethylbenzidine as electrochemical substrate for horseradish peroxidase based enzyme immunoassays. A comparative study, Analyst 123 (1998) 1303–1307, https://doi.org/10.1039/a800255j.
[148] F. Wang, Y. Feng, S. He, L. Wang, M. Guo, Y. Cao, Y. Wang, Y. Yu, Nickel nanoparticles-loaded three-dimensional porous magnetic graphene-like material for non-enzymatic glucose sensing, Microchem. J. 155 (2020), 104748, https://doi.org/10.1016/j.microc.2020.104748.

[149] H. Ehzari, M. Amiri, M. Safari, Enzyme-free sandwich-type electrochemical immunosensor for highly sensitive prostate specific antigen based on conjugation of quantum dots and antibody on surface of modified glassy carbon electrode with core–shell magnetic metal-organic frameworks, Talanta 210 (2020), 120641, https://doi.org/10.1016/j.talanta.2019.120641.

[150] M. Baghayeri, M. Nodehi, A. Amiri, N. Amirzadeh, R. Behazin, M.Z. Iqbal, Electrode designed with a nanocomposite film of CuO Honeycombs/Ag nanoparticles electrogenerated on a magnetic platform as an amperometric glucose sensor, Anal. Chim. Acta 1111 (2020) 49–59, https://doi.org/10.1016/j.aca.2020.03.039.

[151] J.A.R.R. Guivar, E.G.R. Fernandes, V. Zucolotto, A peroxidase biomimetic system based on Fe_3O_4 nanoparticles in non-enzymatic sensors, Talanta 141 (2015) 307–314, https://doi.org/10.1016/j.talanta.2015.03.017.

[152] M. Sharafeldin, G.W. Bishop, S. Bhakta, A. El-Sawy, S.L. Suib, J.F. Rusling, Fe_3O_4 nanoparticles on graphene oxide sheets for isolation and ultrasensitive amperometric detection of cancer biomarker proteins, Biosens. Bioelectron. 91 (2017) 359–366, https://doi.org/10.1016/j.bios.2016.12.052.

[153] B.V. Chikkaveeraiah, V. Mani, V. Patel, J.S. Gutkind, J.F. Rusling, Microfluidic electrochemical immunoarray for ultrasensitive detection of two cancer biomarker proteins in serum, Biosens. Bioelectron. 26 (2011) 4477–4483, https://doi.org/10.1016/j.bios.2011.05.005.

[154] C.A. Proença, T.A. Baldo, T.A. Freitas, E.M. Materón, A. Wong, A.A. Durán, M. E. Melendez, G. Zambrano, R.C. Faria, Novel enzyme-free immunomagnetic microfluidic device based on $Co0._{25}Zn_{0.75}Fe_2O_4$ for cancer biomarker detection, Anal. Chim. Acta 1071 (2019) 59–69, https://doi.org/10.1016/j.aca.2019.04.047.

[155] C.M. Miyazaki, F.M. Shimizu, M. Ferreira, Surface plasmon resonance (SPR) for sensors and biosensors. Nanocharacterization Tech., Elsevier, 2017, pp. 183–200, https://doi.org/10.1016/B978-0-323-49778-7.00006-0.

[156] K. Tamada, Surface plasmon resonance. Compendium of Surface and Interface Analysis, Springer Singapore, Singapore, 2018, pp. 673–678, https://doi.org/10.1007/978-981-10-6156-1_109.

[157] E. Kretschmann, H. Raether, Notizen: radiative decay of non radiative surface plasmons excited by light, Zeitschrift Für Naturforschung A 23 (1968) 2135–2136, https://doi.org/10.1515/zna-1968-1247.

[158] J. Homola, Present and future of surface plasmon resonance biosensors, Anal. Bioanal. Chem. 377 (2003) 528–539, https://doi.org/10.1007/s00216-003-2101-0.

[159] S. Mohammadzadeh-Asl, A. Keshtkar, J. Ezzati Nazhad Dolatabadi, M. de la Guardia, Nanomaterials and phase sensitive based signal enhancment in surface plasmon resonance, Biosens. Bioelectron. 110 (2018) 118–131, https://doi.org/10.1016/j.bios.2018.03.051.

[160] Y. Teramura, Y. Arima, H. Iwata, Surface plasmon resonance-based highly sensitive immunosensing for brain natriuretic peptide using nanobeads for signal amplification, Anal. Biochem. 357 (2006) 208–215, https://doi.org/10.1016/j.ab.2006.07.032.

[161] Y. Sun, Y. Bai, D. Song, X. Li, L. Wang, H. Zhang, Design and performances of immunoassay based on SPR biosensor with magnetic microbeads, Biosens. Bioelectron. 23 (2007) 473–478, https://doi.org/10.1016/j.bios.2007.06.016.

[162] H. Chen, F. Qi, H. Zhou, S. Jia, Y. Gao, K. Koh, Y. Yin, Fe_3O_4@Au nanoparticles as a means of signal enhancement in surface plasmon resonance spectroscopy for thrombin detection, Sens. Actuators B Chem. 212 (2015) 505–511, https://doi.org/10.1016/j.snb.2015.02.062.

[163] N. Filipczak, J. Pan, S.S.K. Yalamarty, V.P. Torchilin, Recent advancements in liposome technology, Adv. Drug Deliv. Rev. 156 (2020) 4–22, https://doi.org/10.1016/j.addr.2020.06.022.

[164] R.P. Liang, G.H. Yao, L.X. Fan, J.D. Qiu, Magnetic Fe_3O_4@Au composite-enhanced surface plasmon resonance for ultrasensitive detection of magnetic nanoparticle-enriched α-fetoprotein, Anal. Chim. Acta 737 (2012) 22–28, https://doi.org/10.1016/j.aca.2012.05.043.

[165] L. Wang, Y. Sun, J. Wang, J. Wang, A. Yu, H. Zhang, D. Song, Preparation of surface plasmon resonance biosensor based on magnetic core/shell Fe_3O_4/SiO_2 and Fe_3O_4/Ag/SiO_2 nanoparticles, Colloids Surf. B Biointerfaces 84 (2011) 484–490, https://doi.org/10.1016/j.colsurfb.2011.02.003.

[166] A.T. Reiner, S. Fossati, J. Dostalek, Biosensor platform for parallel surface plasmon-enhanced epifluorescence and surface plasmon resonance detection, Sens. Actuators B Chem. 257 (2018) 594–601, https://doi.org/10.1016/j.snb.2017.10.116.

[167] S.D. Soelberg, R.C. Stevens, A.P. Limaye, C.E. Furlong, Surface plasmon resonance detection using antibody-linked magnetic nanoparticles for analyte capture, purification, concentration, and signal amplification, Anal. Chem. 81 (2009) 2357–2363, https://doi.org/10.1021/ac900007c.

[168] S.D. Soelberg, R.C. Stevens, A.P. Limaye, C.E. Furlong, Surface plasmon resonance detection using antibody-linked magnetic nanoparticles for analyte capture, purification, concentration, and signal amplification, Anal. Chem. 81 (2009) 2357–2363, https://doi.org/10.1021/ac900007c.

[169] H. Zhang, Y. Sun, J. Wang, J. Zhang, H. Zhang, H. Zhou, D. Song, Preparation and application of novel nanocomposites of magnetic-Au nanorod in SPR biosensor, Biosens. Bioelectron. 34 (2012) 137–143, https://doi.org/10.1016/j.bios.2012.01.032.

[170] J. Wang, Y. Sun, L. Wang, X. Zhu, H. Zhang, D. Song, Surface plasmon resonance biosensor based on Fe_3O_4/Au nanocomposites, Colloids Surf. B Biointerfaces 81 (2010) 600–606, https://doi.org/10.1016/j.colsurfb.2010.08.007.

[171] A.T. Reiner, N.G. Ferrer, P. Venugopalan, R.C. Lai, S.K. Lim, J. Dostálek, Magnetic nanoparticle-enhanced surface plasmon resonance biosensor for extracellular vesicle analysis, Analyst 142 (2017) 3913–3921, https://doi.org/10.1039/C7AN00469A.

[172] Y. Wang, W. Knoll, J. Dostalek, Bacterial pathogen surface plasmon resonance biosensor advanced by long range surface plasmons and magnetic nanoparticle assays, Anal. Chem. 84 (2012) 8345–8350, https://doi.org/10.1021/ac301904x.

[173] Y. Wang, J. Dostalek, W. Knoll, Magnetic nanoparticle-enhanced biosensor based on grating-coupled surface plasmon resonance, Anal. Chem. 83 (2011) 6202–6207, https://doi.org/10.1021/ac200751s.

[174] S. Szunerits, J. Spadavecchia, R. Boukherroub, Surface plasmon resonance: signal amplification using colloidal gold nanoparticles for enhanced sensitivity, Rev. Anal. Chem. 33 (2014) 153–164, https://doi.org/10.1515/revac-2014-0011.

[175] L.A. Lyon, M.D. Musick, M.J. Natan, Colloidal Au-enhanced surface plasmon resonance immunosensing, Anal. Chem. 70 (1998) 5177–5183, https://doi.org/10.1021/ac9809940.

[176] X. Liu, Y. Hu, S. Zheng, Y. Liu, Z. He, F. Luo, Surface plasmon resonance immunosensor for fast, highly sensitive, and in situ detection of the magnetic nanoparticles-enriched Salmonella enteritidis, Sens. Actuators B Chem. 230 (2016) 191–198, https://doi.org/10.1016/j.snb.2016.02.043.

[177] S. Krishnan, V. Mani, D. Wasalathanthri, C.V. Kumar, J.F. Rusling, Attomolar detection of a cancer biomarker protein in serum by surface plasmon resonance using superparamagnetic particle labels, Angew. Chem. Int. Ed. 50 (2011) 1175–1178, https://doi.org/10.1002/anie.201005607.

[178] J. Wang, Z. Zhu, A. Munir, H.S. Zhou, Fe_3O_4 nanoparticles-enhanced SPR sensing for ultrasensitive sandwich bio-assay, Talanta 84 (2011) 783–788, https://doi.org/10.1016/j.talanta.2011.02.020.

[179] S. Li, Q. Wu, P. Ma, Y. Zhang, D. Song, X. Wang, Y. Sun, A sensitive SPR biosensor based on hollow gold nanospheres and improved sandwich assay with PDA-Ag@Fe_3O_4/rGO, Talanta 180 (2018) 156–161, https://doi.org/10.1016/j.talanta.2017.12.051.

[180] M. Dolci, J.F. Bryche, C. Leuvrey, S. Zafeiratos, S. Gree, S. Begin-Colin, G. Barbillon, B.P. Pichon, Robust clicked assembly based on iron oxide nanoparticles for a new type of SPR biosensor, J. Mater. Chem. C 6 (2018) 9102–9110, https://doi.org/10.1039/C8TC01166D.

[181] F. Zou, X. Wang, F. Qi, K. Koh, J. Lee, H. Zhou, H. Chen, Magneto-plamonic nanoparticles enhanced surface plasmon resonance TB sensor based on recombinant gold binding antibody, Sens. Actuators B Chem. 250 (2017) 356–363, https://doi.org/10.1016/j.snb.2017.04.162.

[182] J. He, M. Huang, D. Wang, Z. Zhang, G. Li, Magnetic separation techniques in sample preparation for biological analysis: a review, J. Pharm. Biomed. Anal. 101 (2014) 84–101, https://doi.org/10.1016/j.jpba.2014.04.017.

[183] Y. Jia, Y. Peng, J. Bai, X. Zhang, Y. Cui, B. Ning, J. Cui, Z. Gao, Magnetic nanoparticle enhanced surface plasmon resonance sensor for estradiol analysis, Sens. Actuators B Chem. 254 (2018) 629–635, https://doi.org/10.1016/j.snb.2017.07.061.

[184] C.A. Proença, T.A. Freitas, T.A. Baldo, E.M. Materón, F.M. Shimizu, G.R. Ferreira, F.L.F. Soares, R.C. Faria, O.N. Oliveira, Use of data processing for rapid detection of the prostate-specific antigen biomarker using immunomagnetic sandwich-type sensors, Beilstein J. Nanotechnol. 10 (2019) 2171–2181, https://doi.org/10.3762/bjnano.10.210.

[185] F. Soetaert, P. Korangath, D. Serantes, S. Fiering, R. Ivkov, Cancer therapy with iron oxide nanoparticles : agents of thermal and immune therapies, Adv. Drug Deliv. Rev. 163–164 (2020) 65–83, https://doi.org/10.1016/j.addr.2020.06.025.

[186] Y. Abo-zeid, N.S.M. Ismail, G.R. McLean, N.M. Hamdy, A molecular docking study repurposes FDA approved iron oxide nanoparticles to treat and control COVID-19 infection, Eur. J. Pharm. Sci. 153 (2020), 105465, https://doi.org/10.1016/j.ejps.2020.105465.

[187] J. Zhong, E.L. Rösch, T. Viereck, M. Schilling, F. Ludwig, Toward rapid and sensitive detection of SARS-CoV-2 with functionalized magnetic nanoparticles, ACS Sensors 6 (2021) 976–984, https://doi.org/10.1021/acssensors.0c02160.

[188] S.K. Jat, H.A. Gandhi, J. Bhattacharya, M.K. Sharma, Magnetic nanoparticles: an emerging nano-based tool to fight against viral infections, Mater. Adv. 2 (2021) 4479–4496, https://doi.org/10.1039/D1MA00240F.

[189] S.B. Somvanshi, P.B. Kharat, T.S. Saraf, S.B. Somwanshi, S.B. Shejul, K.M. Jadhav, Multifunctional nano-magnetic particles assisted viral RNA-extraction protocol for potential detection of COVID-19, Mater. Res. Innov. 25 (2021) 169–174, https://doi.org/10.1080/14328917.2020.1769350.

[190] N.S. El-Gendy, H.N. Nassar, Biosynthesized magnetite nanoparticles as an environmental opulence and sustainable wastewater treatment, Sci. Total Environ. 774 (2021), 145610, https://doi.org/10.1016/j.scitotenv.2021.145610.